

~~SECRET~~

Copy
RM E58D15a

CLASSIFICATION CHANGED

Copy 2

UNCLASSIFIED

NACA

authority of *NASA memo dated July 17, 1963,*
s/P.M. Lovell, Jr. *NSR - 8-5-63.*

RESEARCH MEMORANDUM

COMBUSTION OF GASEOUS HYDROGEN IN A SMALL
RECTANGULAR RAMJET COMBUSTOR

By John W. Sheldon

Lewis Flight Propulsion Laboratory
Cleveland, Ohio

~~CLASSIFICATION CHANGED~~

~~CONFIDENTIAL~~

To _____

By authority of *NASA PA#7* Date *June 2, 1958*
effective date May 29, 1958. *by JBE*

1.N.58-990

AUG 25 1958

~~CLASSIFIED DOCUMENT~~

~~This material contains information affecting the National Defense of the United States within the meaning of the espionage laws, Title 18, U.S.C., Secs. 793 and 794, the transmission or revelation of which in any manner to an unauthorized person is prohibited by law.~~

**NATIONAL ADVISORY COMMITTEE
FOR AERONAUTICS**

WASHINGTON
August 25, 1958

~~SECRET~~

~~CONFIDENTIAL~~

Classified Files
NACA LIBRARY

LANGLEY AERONAUTICAL LABORATORY
Langley Field, Va.

~~CONFIDENTIAL~~~~SECRET~~

NASA Technical Library



3 1176 01435 9187

NATIONAL ADVISORY COMMITTEE FOR AERONAUTICS

RESEARCH MEMORANDUM

COMBUSTION OF GASEOUS HYDROGEN IN A SMALL RECTANGULAR RAMJET COMBUSTOR*

By John W. Sheldon

SUMMARY

Seven fuel-injector-flameholder configurations were investigated in a rectangular ramjet combustor having a cross section of 1 by 6 inches. Combustion efficiencies were determined for a range of fuel-air equivalence ratios at the following combustor-inlet conditions: total pressure, 15 inches of mercury absolute; Mach number, 0.24; total temperature, 80° F. Combustor-inlet pressures resulting in blowout of the flame were also determined for a range of fuel-air equivalence ratios.

For the combustor configurations and test conditions investigated, the maximum combustion efficiency obtained was 90 percent. The small combustor size appeared to have an adverse effect on performance, probably because of flame-quenching on some of the combustor surfaces. Large-scale hydrogen combustors that have demonstrated satisfactory performance at similar operating conditions did not produce acceptable performance when scaled down to the dimensions of this combustor.

INTRODUCTION

The possibility of improving the range of jet-propelled aircraft by using high-energy fuels is being investigated at the NACA Lewis laboratory (ref. 1). To exploit fully the potential of special fuels, such as hydrogen, short combustors should be developed to take advantage of their high reactivity and thus reduce engine size and weight. Engine weight is especially important at the high altitudes presently being considered for missile flight paths. For instance, using the Breguet range equation, at 110,000 feet and a flight Mach number of 4.0, only a 4-percent reduction in engine weight will extend the range about 1 percent, whereas, at 70,000 feet, a 16-percent weight reduction is required to produce the same gain in range.

It has been demonstrated that ramjet combustors may be shortened by the use of hydrogen fuel (refs. 2 and 3). The various combustion properties of hydrogen presented in reference 4 indicate that some types of small combustor units give high performance with hydrogen fuel.

*Title, Confidential.

N A C A LIBRARY

LANGLEY AERONAUTICAL LABORATORY
Langley Field, Va.~~SECRET~~
~~CONFIDENTIAL~~

4802

CD-1

AUG 25 1958
I.N. 58-990

Classified Files

The investigation reported herein determines the design principles for a small, rectangular combustor having a 1- by 6-inch cross section and a $6\frac{1}{2}$ -inch burning length. One use for such a combustor would be in a cascaded (multiple parallel units) ramjet engine as in reference 5. Combustion efficiency was determined for seven fuel-injector-flameholder combinations at the following approximate combustor-inlet conditions: total pressure, 15 inches of mercury absolute; Mach number, 0.24; and total temperature, 80° F. These combustor-inlet conditions simulate combustor operation for the cascaded ramjet engine of reference 5 in one of the NACA small supersonic wind tunnels at a Mach number of 3.0. If a ramjet engine were operated at a flight Mach number of 3.0 above the tropopause, the burner-inlet pressure and Mach number would be the same, but the total temperature would be about 630° F. The effects of combustor pressure and Mach number on flame blowout were also determined for each fuel-injection system.

4802

APPARATUS

Connected-Pipe Combustor Facility

The rectangular ramjet combustor was tested in the connected-pipe facility shown in figure 1. Combustion air and altitude exhaust were supplied by the laboratory air supply system. The combustion air was throttled and then metered by an ASME standard orifice. A bundle of flow straightening tubes was installed upstream of the orifice to reduce the required length of the orifice run.

A $13\frac{1}{2}$ -foot length of 12-inch pipe downstream of the combustor served as a calorimeter for the determination of combustion efficiency. The temperature of the exhaust gases in the calorimeter was kept between 400° and 500° F by spraying water into the exhaust gases when necessary. Two thermocouple rakes measured the equilibrium temperatures at the exit of the calorimeter. The pressure level in the calorimeter, as well as the combustor, was controlled by a throttle valve in the altitude exhaust system.

Rectangular Combustor

The rectangular combustor and transition section are illustrated in figure 2. The fuel-injector-flameholder was located $1\frac{1}{2}$ inches downstream of the convergent transition section. The combustor length was $6\frac{1}{2}$ inches, measured from the fuel injector to the primary water spray, which was located at the combustor exit to quench the combustion reaction. The combustor length was assumed to end at the primary quench water spray even for the data points which used no quench water; this assumption is subject to question, as discussed in appendix B. The combustor was cooled externally by air jets directed on its top and bottom surfaces.

The velocities measured at the combustor inlet are shown in figure 3. The combustor-inlet conditions were approximately the same as those at which the combustion efficiency data were obtained. The velocity profile was comparatively flat, varying less than ± 5 percent from the average value of 268 feet per second.

Fuel-Injector-Flameholder Configurations

The seven fuel-injector-flameholder configurations tested are shown in figure 4. The pertinent features of each configuration are summarized in table I.

Fuel System

The gaseous-hydrogen fuel was supplied from cylinders at an initial pressure of 2400 pounds per square inch gage and was passed through a pressure-reducing valve and a sonic-flow metering orifice to the fuel injector. Variation of the fuel weight flow was obtained by varying the pressure upstream of the sonic-flow orifice.

Instrumentation

The airflow was measured by the orifice run shown in figure 1. The differential pressure was indicated on a U-tube manometer, and the line pressure was indicated on an absolute manometer.

The fuel flow was measured by a calibrated sonic-flow orifice. The pressure upstream of this orifice was indicated on a Bourdon tube gage. Temperatures in the fuel and combustion-air lines were measured by iron-constantan thermocouples. The gas temperature at the calorimeter exit was measured by 19 Chromel-Alumel thermocouples in two rakes. The calorimeter wall temperature was measured by four iron-constantan thermocouples at circumferential stations 90° apart at the axial station of the thermocouple rakes. All temperatures were indicated on nonrecording self-balancing potentiometers.

PROCEDURE

Combustor Operating Conditions

The various configurations were compared on the basis of combustion efficiency at the following operating conditions:

Inlet air pressure, in. Hg abs	14.7±1.7
Inlet air total temperature, °F	84±14
Inlet air Mach number	0.24±0.04
Equivalence ratio	0.08 to 0.53

These values correspond approximately to the combustor-inlet conditions in a ramjet tested in one of the NACA small supersonic wind tunnels operating at Mach 3.0 and an ambient pressure equivalent to an 80,000-foot altitude.

Combustor-Inlet Velocity Profile

The velocity survey was made at the combustor-inlet cross section. The fuel-injector-flameholder configuration was replaced by a six-tube total-pressure rake at each of three stations across the 1-inch dimension of the duct. The total pressures, indicated by manometers, were recorded at the combustor-inlet conditions at which the combustion efficiency data were obtained. Wall static pressure was measured in the plane of the total-pressure survey. From this static pressure and the total pressure measured at a given point, the local Mach number was determined. The local velocity was then readily obtained from this Mach number and the inlet total temperature.

Combustion Efficiency

Combustion efficiency was determined over a range of equivalence ratio for each configuration. Equivalence ratio is the metered fuel-air ratio divided by the stoichiometric fuel-air ratio of 0.0294 for hydrogen. After combustion was established, a fuel-flow rate was selected, and the combustor-inlet conditions were set. Quench water was added as needed, first through the primary sprays and then through the secondary sprays to keep the calorimeter rake temperature between 400° and 500° F. The ratio of the measured enthalpy rise in the calorimeter to the theoretical heating value of the fuel is defined as combustion efficiency. All symbols are defined in appendix A, and a more detailed analysis of the method of computing combustion efficiency is presented in appendix B.

Combustor Blowout Pressure

Combustor blowout pressure was determined for a range of equivalence ratios, with the burner-inlet airflow and temperature held constant. An airflow of 0.4 pound per second was chosen because it corresponds to a ramjet operating supercritically at the wind tunnel conditions. Because of safety restrictions, the maximum equivalence ratio at which blowout data were obtained was in general about 0.30.

After combustion was established at the combustion efficiency test conditions, the burner pressure was lowered until blowout occurred. Mach number was calculated from the burner static pressure at blowout and the airflow at the combustor inlet. The total pressure at blowout was then obtained from Mach number and static pressure.

RESULTS

Combustion Efficiency

Initial tests were conducted using a simple spray bar (1/4 in. diam.) as fuel injector and flameholder. This configuration would not stabilize the combustion at the test conditions. Modifications in orifice size (0.026- to 0.067-in. diam.), spacing, and orientation were not sufficient to provide the required stability; consequently, more complex systems were explored.

Configuration A. - A maximum combustion efficiency of 80 percent was obtained with the scaled-down version of a swirl can used in reference 6. Figure 5 shows the combustion efficiency increasing with equivalence ratio until blowout occurred at an equivalence ratio of 0.30.

Configuration B. - By using a shrouded, flattened spray bar similar to that of reference 7, scattered efficiency data were obtained as shown in figure 6. Although efficiency as high as 87 percent was obtained with this configuration, combustion was unstable. Rich blowout occurred at an equivalence ratio of 0.29. The fuel jets on the fuel supply side of the injector were alternately blowing out and relighting. No evidence of burning was visible inside the injector shroud.

Configuration C. - The combustion efficiency increased with increasing equivalence ratio, reaching a maximum of 78 percent (fig. 7). During operation at an equivalence ratio of 0.08 the gutters were heated to incandescence. As fuel flow and, consequently, equivalence ratio increased, the incandescence faded. Just prior to blowout (equivalence ratio of 0.24), the combustor appeared dark.

Configuration D. - Figure 8 shows the combustion efficiency reaching a peak value of 77 percent at an equivalence ratio of 0.29 and then decreasing to blowout at an equivalence ratio of 0.42.

Configuration E. - A decrease in fuel-injection velocity by doubling the number of points of injection over those of configuration D raised the peak combustion efficiency to 89 percent (fig. 9) but had little effect on rich-blowout equivalence ratio.

Configuration F. - The combustion efficiency data shown in figure 10 for configuration F were above 85 percent for a range of equivalence ratios from 0.32 to 0.52 at inlet air conditions of pressure, 15 inches of mercury absolute, Mach number, 0.24, and temperature, 80° F. The maximum combustion efficiency, 90 percent, for all configurations tested was achieved by this configuration at an equivalence ratio of 0.52. No blowout was encountered over the range of equivalence ratio covered.

Configuration G. - The admission of air inside the V-gutters of configuration F dropped the combustion efficiency curve about 5 percent at lean equivalence ratios (fig. 11). No blowout was encountered at the combustion efficiency test conditions.

Combustor Blowout Pressure

The combustor-blowout-pressure data are presented in figure 12 for the seven combustor configurations. The variation of combustor blowout pressure with equivalence ratio is observed to follow three distinct patterns. Configurations A, B, and C follow curves of increasing slope (fig. 12(a)). Configurations D and E follow curves with decreasing slopes (fig. 12(b)). The blowout-pressure curves of configuration F and G (fig. 12(b)) have a constant slope at a lower pressure level than the other five configurations. Configurations F and G, which had the best blowout characteristics, also exhibited the best combustion efficiencies.

DISCUSSION

The relatively low combustion efficiencies and the high pressures at which flame blowout occurred can probably be attributed to the small combustor size. Figure 13 (reproduced from ref. 4) shows minimum tube sizes for propagation of hydrogen-air flames as a function of pressure and fuel-air mixture composition. If it is assumed that the tube diameters in figure 13 are indicative of the quenching distances in the combustors studied in this investigation, then it would be concluded that the combustor walls caused very little quenching; but severe quenching may have occurred near the points of flame initiation around the tiny fuel jets. However, if allowance is made for the increase in quenching distance due to turbulence (ref. 4), it appears possible that the flame-holder surfaces and combustor walls may have also exerted some detrimental quenching effects.

It therefore appears likely that flame-quenching resulting from the small combustor size may account for the high blowout pressures and in part for the low combustion efficiencies. It would appear that the low combustion efficiencies could also be attributed in part to inadequate fuel-air mixing in the short-length combustor. Mixing could be improved

by using more sources of fuel injection, but this would result in smaller injectors and even more flame-quenching. The combustor configurations investigated therefore represent compromise designs necessary to provide both adequate mixing and adequate flame stability.

Effect of Design Variables on Combustion Efficiency

Configurations A, B, and C burned at the specified inlet conditions (where a simple spray tube would not burn) but with poor and scattered combustion efficiency. These scattered data seemed to be caused by marginal stabilization characteristics, which indicate that injector configurations like A or B cannot be scaled down this far.

Configurations D and E inject fuel in an entirely different manner, that is, directly downstream at high velocity. The fuel concentration in or near the flameholder would be much less than with configurations A, B, or C, which possibly accounts for the increase in stability. The further increase in combustion efficiency and stability between configurations E and D could have resulted from an increased fuel concentration in the flame stabilizing region. Configuration E with less fuel-injection velocity would have the greater fuel concentration and did have the higher, less scattered, combustion efficiency.

Configurations F and G gave the best combustion efficiency of all the configurations tested. Presumably, the V-gutters provided a piloting zone neither too rich, as in configurations A, B, or C, nor too lean, as in configurations D or E. In addition, the shape of the combustion efficiency curves (increasing combustion efficiency with increasing equivalence ratio) indicates that good fuel-air mixing occurred with maximum combustion efficiency realized as a stoichiometric fuel-air ratio is approached. The mixing may be too vigorous at lower equivalence ratios and probably causes dilution-quenching, which would account for the combustion efficiency falloff. Configurations F and G differed in that a small amount of air was admitted through a hole in the V-gutter for configuration G. The difference in combustion efficiency, if significant, was that the combustion efficiency of configuration G was 5 percent lower at low equivalence ratios, possibly because of greater dilution-quenching.

Effect of Design Variables on Blowout Limits

Configurations A, B, and C inject fuel against and inside a cold flameholder wall. Figure 13 (reproduced from ref. 4) shows that quenching diameter is a function of pressure and equivalence ratio. If blowout were a result of wall-quenching or a local rich flammability limit, increasing the equivalence ratio in a zone that was already over stoichiometric would increase the blowout pressure. A sharply increasing blowout

pressure in the higher equivalence ratios was observed for configurations A, B, and C (fig. 12(a)), which indicates that a combination of wall-quenching within the flameholder and of a local rich blowout limit probably was controlling the blowout.

Configurations D and E inject fuel downstream at a high velocity thereby causing the region inside the gutter to have a lower local equivalence ratio. Increasing equivalence ratio has only a slightly increasing effect on blowout pressure for these configurations (fig. 12(b)). It can be assumed that because of the fuel-injection direction a rich blowout limit was not reached locally and that blowout was more a result of wall-quenching within the flameholder.

The blowout pressures for configurations F and G were lower than those of D and E, but the curves were of similar slopes (fig. 12(b)). The lower blowout pressure can be attributed to the greater width of the V-gutter with its larger effective turbulent wake or to a better local equivalence ratio within the stabilizing region. The similarity of slopes leads to the same conclusion that the local equivalence ratio in the V-gutter did not exceed the rich blowout limit. It seems likely then that a small amount of fuel diffused from the jet and burned while still within the V-gutter. The greater portion of the fuel impinged on the combustor wall and was deflected or fanned out sideways, a phenomenon that should produce good mixing and spreading of the fuel.

SUMMARY OF RESULTS

Seven fuel-injector-flameholder configurations were tested in a 1- by 6-inch rectangular combustor $6\frac{1}{2}$ inches long. The results are as follows:

1. The best configuration (configuration F) produced combustion efficiencies over 85 percent for equivalence ratios from 0.32 to 0.52 at the following inlet air conditions: a pressure of 15 inches of mercury absolute, a Mach number of 0.24, and a temperature of 80° F.
2. This same configuration also had the best flame stability, blowing out at a pressure of $10\frac{1}{2}$ inches of mercury absolute and a Mach number of 0.57 for a range of equivalence ratios from 0.08 to 0.27.
3. Several hydrogen combustors that had previously provided high performance at comparable conditions were reproduced on the small scale necessary to fit into the 1- by 6-inch duct. One of these configurations gave no combustion; the others showed marginal stability and low

combustion efficiency. The poor performance was probably due to a quenching effect, either inside the flameholder or in the stream itself.

Lewis Flight Propulsion Laboratory
National Advisory Committee for Aeronautics
Cleveland, Ohio, April 28, 1958

4802

CD-2

APPENDIX A

SYMBOLS

C_p	heat capacity, Btu/lb, °F
ΔH_a	enthalpy rise of combustion air, Btu/sec
ΔH_B	lower heat of combustion of hydrogen, Btu/lb
ΔH_f	enthalpy rise of fuel, Btu/sec
ΔH_{qa}	enthalpy rise of quench air, Btu/sec
ΔH_v	enthalpy of steam at temperature T_Q , referenced to liquid water at 32° F, Btu/lb
ΔH_w	enthalpy rise of quench water, Btu/sec
Q_b	heat lost from burner wall to room air, Btu/sec
Q_C	heat lost from calorimeter to room by convection, Btu/sec
Q_j	heat transferred to water jacket, Btu/sec
Q_P	heat gained (+) or lost (-) by calorimeter piping, Btu/sec
T_a	air inlet temperature, °F
T_f	fuel inlet temperature, °F
T_{ji}	temperature of water entering water jacket, °F
T_{jo}	temperature of water leaving water jacket, °F
T_P	calorimeter pipe temperature, °F
T_Q	gas temperature at calorimeter exit, °F
T_w	water inlet temperature, °F
t	time, sec
W_a	combustion airflow rate, lb/sec
W_f	fuel-flow rate, lb/sec

W_j water-flow rate to water jacket, lb/sec
 W_{qa} quench airflow rate, lb/sec
 W_w quench water-flow rate, lb/sec
 η_B combustion efficiency

4802

CD-2 back

APPENDIX B

HEAT-BALANCE COMBUSTION EFFICIENCY

Combustion Termination

The combustion length was assumed to end where the quench-water spray was added. Reference 8 shows data where combustion efficiency remained constant while the amount of quench water varied, which thus indicates that the reaction was quenched independently of the water-flow rate. However, no quench water could be added below an equivalence ratio of about 0.28 because of low combustion efficiency and fuel flow. Since quench water was not added, the actual burning length may have been longer than the combustor length. In general, the data points with no quench water are of less interest because they are already points of low combustion efficiency. The fact that the combustion efficiency curves blend smoothly (such as fig. 10) from data taken with no quench water to data taken with quench water indicated that the combustion was completed or terminated by the same point (primary quench-water station) for both cases. The open symbols are data where no quench water was added, and the solid symbols are with quench water.

4802

Calculation Method

The heat-balance method of measuring combustion efficiency consists simply of adding the measured rise in enthalpy of the combustor-calorimeter flow system to the heat lost to the surroundings from the flow system and comparing this sum to the theoretical heat released by complete combustion of the fuel.

The flow system consists of combustion air, gaseous-hydrogen fuel, air for aspirating the secondary water spray bars, and water for the primary and secondary water spray bars. The combustor and calorimeter piping are considered surroundings and not part of the flow system (see fig. 14).

It is assumed that the reactants (fuel and combustion air) are raised to the calorimeter-exit temperature, at which the reaction occurs. The assumption eliminates the need to know the heat capacity of the products. The enthalpy rise of the combustion air is

$$\Delta H_a = W_a 0.25 (T_Q - T_a)$$

where $C_p = 0.25$ for air (ref. 9).

The enthalpy rise of the fuel is given by

$$\Delta H_F = W_F 3.5 (T_Q - T_F)$$

where $C_p = 3.5$ for hydrogen (ref. 9).

The enthalpy change of the air to the secondary spray bar is given by

$$\Delta H_{qa} = W_{qa} 0.25 (T_Q - T_a)$$

The enthalpy rise of the quench water is

$$\Delta H_W = W_W [\Delta H_V - (T_W - 32)]$$

where ΔH_V is the steam enthalpy at temperature T_Q (ref. 10).

Heat flows to or from the surroundings by four processes. Heat is removed from the system by cooling water in a water jacket at the combustor exit. Heat is gained or lost in the calorimeter piping because the pipe temperature is not at equilibrium with the exhaust gases. Heat is lost by convection from the calorimeter piping to the room air. The combustor walls also give up heat by both forced convection and radiation.

The heat removed through the water jacket may be expressed as

$$Q_j = W_j (T_{j0} - T_{j1})$$

The change in heat content of the calorimeter piping is

$$Q_p = 111 \frac{\Delta T_p}{t}$$

where $\Delta T_p/t$ is the change in calorimeter wall temperature with time and 111 represents the number of Btu's required to raise the calorimeter pipe temperature 1° F. If the wall temperature is increasing, the Q_p term is positive; however, if the wall temperature is decreasing, Q_p is negative.

The calculated heat loss by convection and radiation from the calorimeter pipe Q_C to room air is shown in figure 15 as a function of the pipe wall temperature T_p .

Calculations for the rectangular combustor showed that with forced convection about 3 percent of the combustion heat release was lost through the combustor walls. This 3-percent value is added on to the combustion efficiency.

The theoretical heat release was taken as the lower heat of combustion ΔH_B of gaseous-hydrogen fuel at the calorimeter-exit gas temperature T_Q . The variation of the lower heat of combustion with temperature is shown in figure 16. The curve is a plot of Kirchhoff's integrated equation using heat capacity data from reference 7 and an ΔH_B of -51,571.4 at 77° F.

The combustion efficiency is expressed by

$$\eta_B = \left(\frac{\Delta H_a + \Delta H_f + \Delta H_{qa} + \Delta H_w + Q_j + Q_p + Q_c}{W_f \Delta H_B} \right) 100 + 3$$

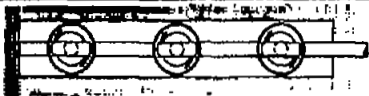

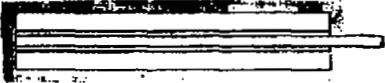



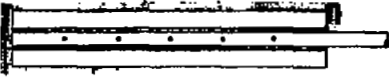

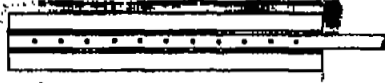

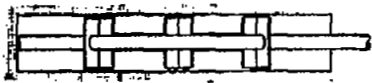

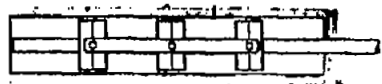

The approximate percentage of the total measured heat release contributed by each of the terms in the heat balance is

Term	Percent of total heat release for a typical data point	
	With quench water	Without quench water
ΔH_a	20.0	49.0
ΔH_f	4.3	5.5
ΔH_{qa}	5.5	12.4
ΔH_w	54.8	0.0
Q_j	4.6	7.7
Q_p	6.0	16.9
Q_c	4.8	8.5
Total	100.0	100.0

REFERENCES

1. Olson, Walter T., and Gibbons, Louis C.: Status of Combustion Research on High-Energy Fuels for Ram Jets. NACA RM E51D23, 1951.
2. Dangle, E. E., and Kerslake, William R.: Experimental Evaluation of Gaseous Hydrogen Fuel in a 16-Inch-Diameter Ram-Jet Engine. NACA RM E55J18, 1955.
3. Cervenka, A. J., and Sheldon, J. W.: Method for Shortening Ram-Jet Engines by Burning Hydrogen Fuel in the Subsonic Diffuser. NACA RM E56G27, 1956.
4. Drell, Isadore L., and Belles, Frank E.: Survey of Hydrogen Combustion Properties. NACA RM E57D24, 1957.
5. Woollett, Richard R., and Ferguson, Harold M.: Performance of a Two-Dimensional Cascade Inlet at a Free-Stream Mach Number of 3.05 and Angles of Attack of -3° , 0° , and 6° . NACA RM E57L06, 1958.
6. Rayle, Warren D., Jones, Robert E., and Friedman, Robert: Experimental Evaluation of "Swirl-Can" Elements for Hydrogen-Fuel Combustor. NACA RM E57C18, 1957.
7. Kerslake, William R.: Combustion of Gaseous Hydrogen at Low Pressures in a 35° Sector in a 28-Inch-Diameter Ramjet Combustor. NACA RM E58A21a, 1958.
8. Kerslake, W. R., and Dangle, E. E.: Tests with Hydrogen Fuel in a Simulated Afterburner. NACA RM E56D13a, 1956.
9. Keenan, Joseph H., and Kaye, Joseph: Gas Tables. John Wiley & Sons, Inc., 1948.
10. Keenan, Joseph H., and Keyes, Frederick G.: Thermodynamic Properties of Steam. John Wiley & Sons, Inc., 1936.

TABLE I. - DETAILS OF FUEL-INJECTOR FLAMEHOLDERS

Con- fig- ura- tion	Description	Sketch of configuration looking upstream into combustor	Side view Airflow →	Maximum cross- sectional blockage, percent	Fuel-injection orifices		Direction of fuel injection with respect to airflow	Equiv- alence ratio required to choke injector orifices
					Number	Diameter		
A	Three swirl cans, dimensions scaled from ref. 5			32.6	6	0.055	Normal	0.083
B	Fuel injected from flattened tube in- side an injector shroud - similar to larger scale config- uration reported in ref. 6			37.5	12	0.067	Normal	0.164
C	Fuel injected into V-gutter having gutter extensions sloping downstream			37.5	6	0.067	Upstream	0.137
D	Fuel injected behind injector tube inside a shroud			37.5	5	0.067	Downstream	0.114
E	Fuel injected behind injector tube inside a shroud			37.5	11	0.067	Downstream	0.251
F	Three short V- gutters at right angles to the fuel- injector tube - fuel injected behind each of these three gutters			32.9	6	0.067	Normal	0.137
G	Same as configura- tion F except air is admitted to the three V-gutters			32.1	6	0.067	Normal	0.137

CD-6077

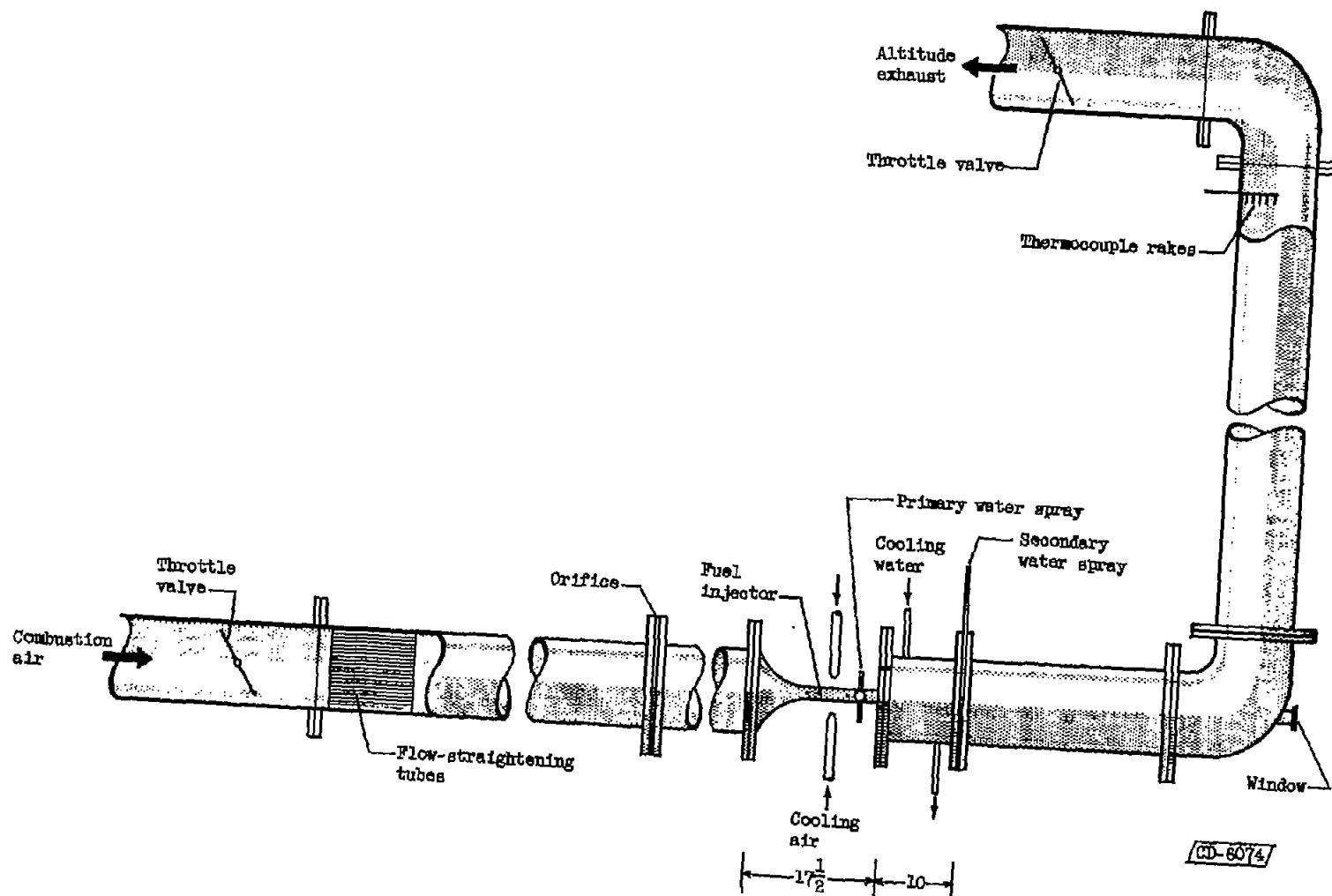


Figure 1. - Connected-pipe installation of 1- by 8-inch rectangular ramjet combustor. (All dimensions in inches.)

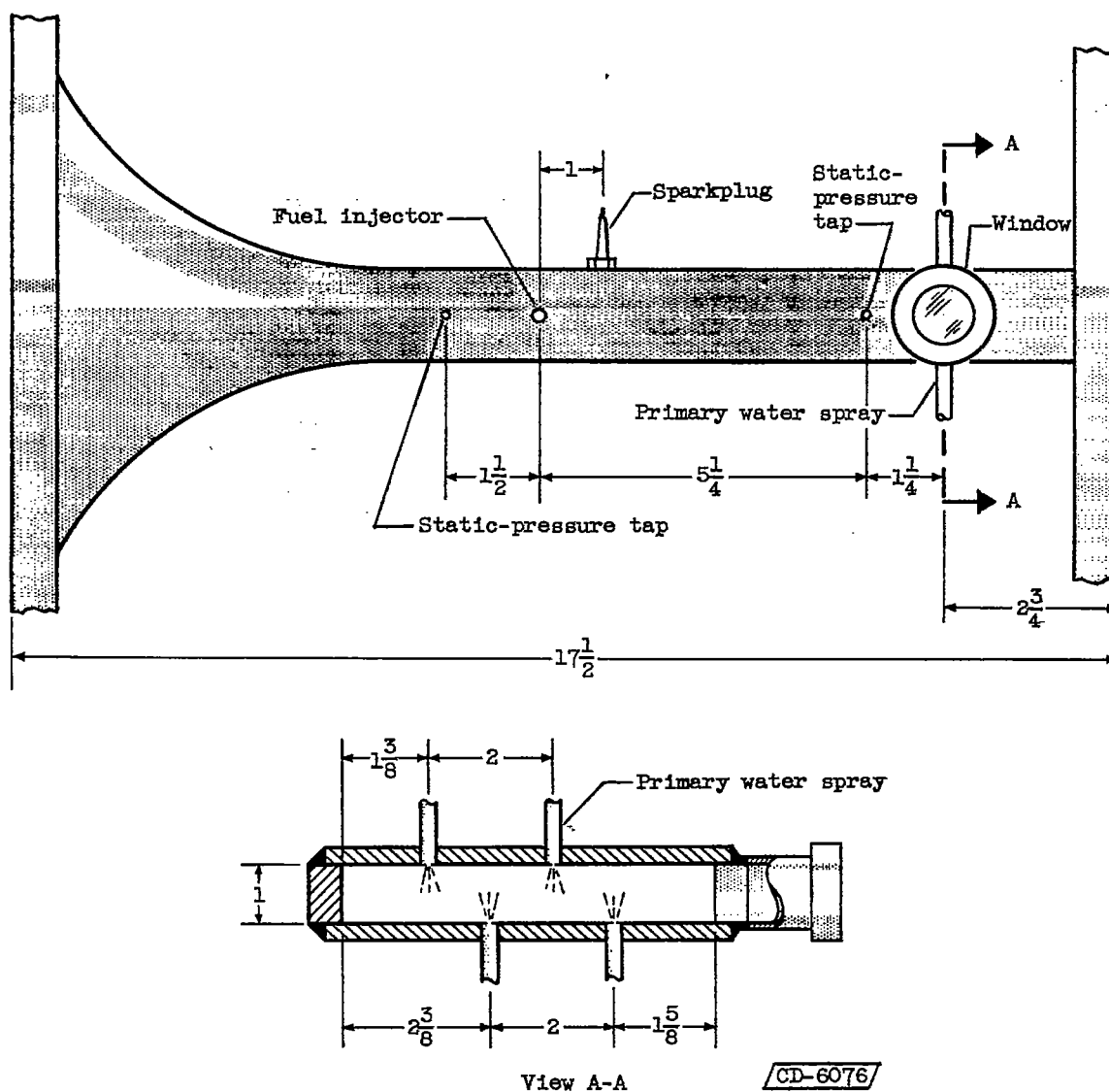
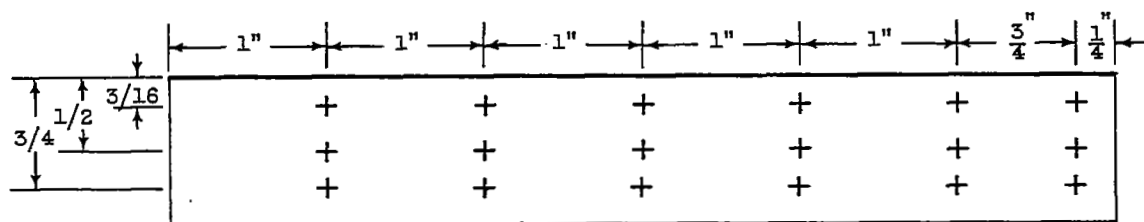


Figure 2. - Detailed view of test section containing 1- by 6-inch rectangular ramjet combustor. (All dimensions in inches.)



Combustor-inlet cross section showing location of velocity measurements

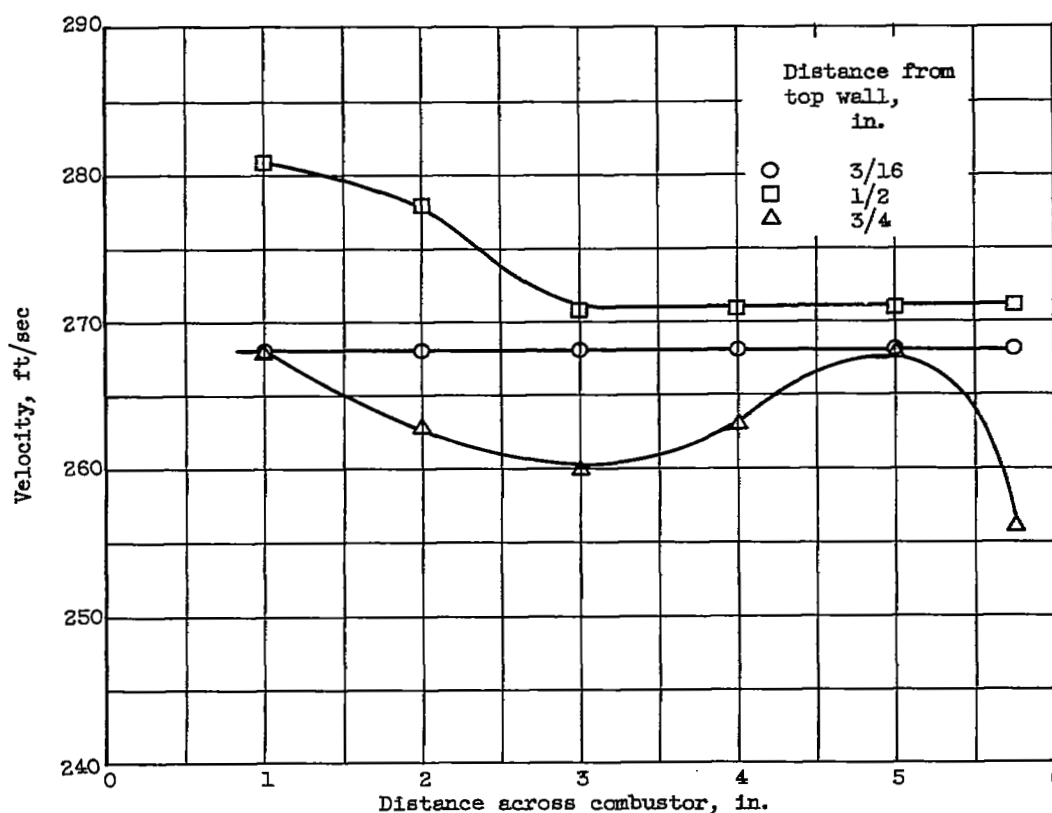
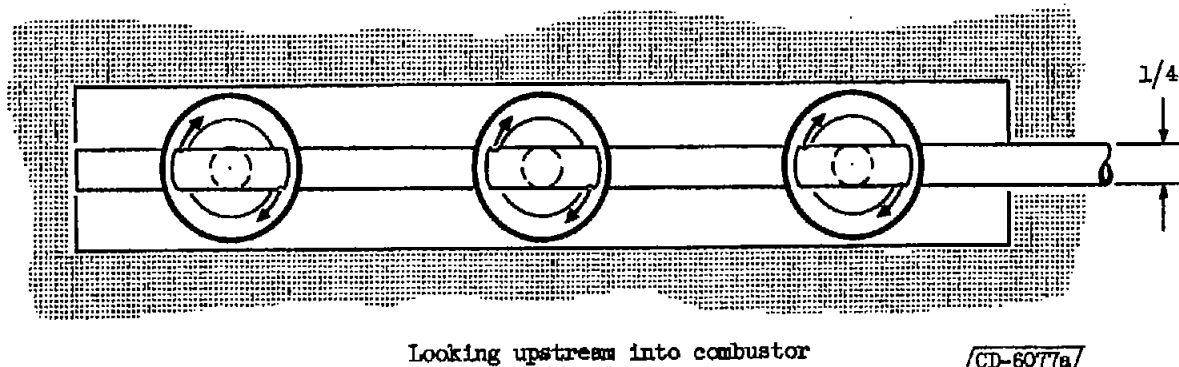
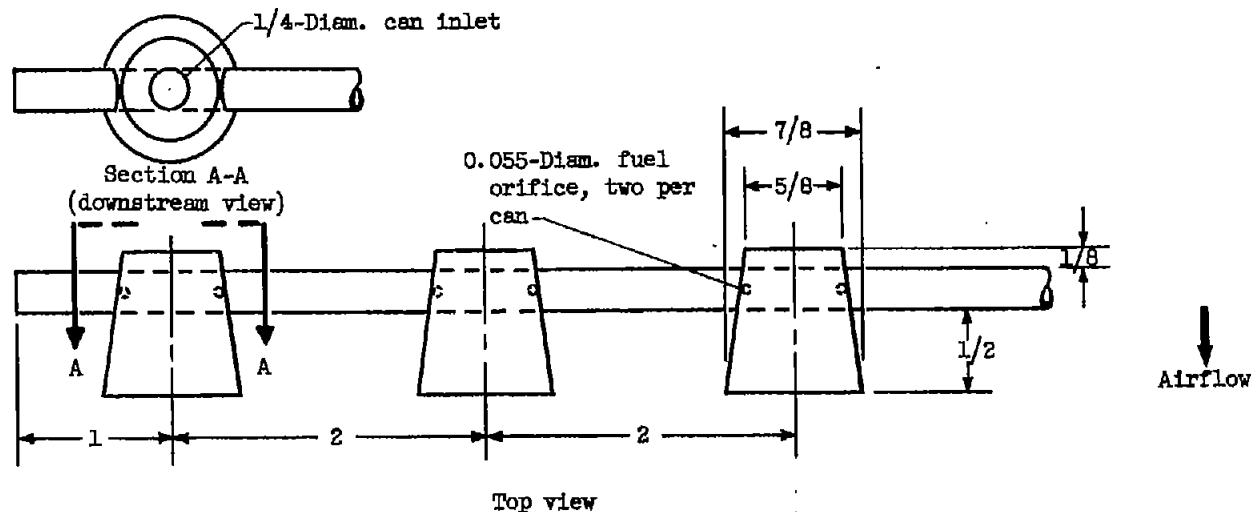
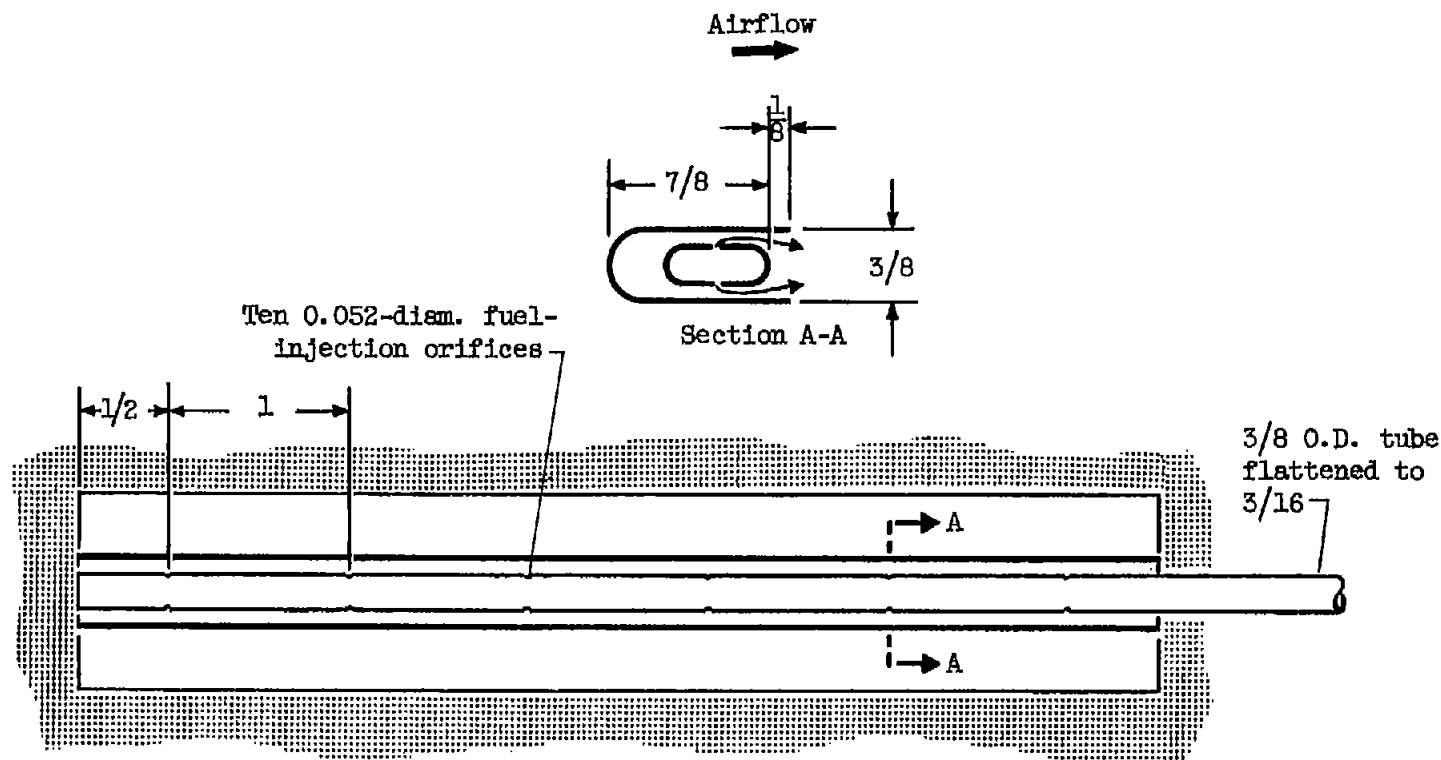


Figure 3. - Combustor-inlet velocity profile. Inlet air weight flow, 0.415 ± 0.005 pound per second; static pressure, 13.93 ± 0.08 inches of mercury; temperature, 85°F .



(a) Configuration A, swirl can installation.

Figure 4. - Details of fuel-injector-flameholder configurations tested in 1- by 6-inch rectangular ramjet combustor. (All dimensions in inches.)

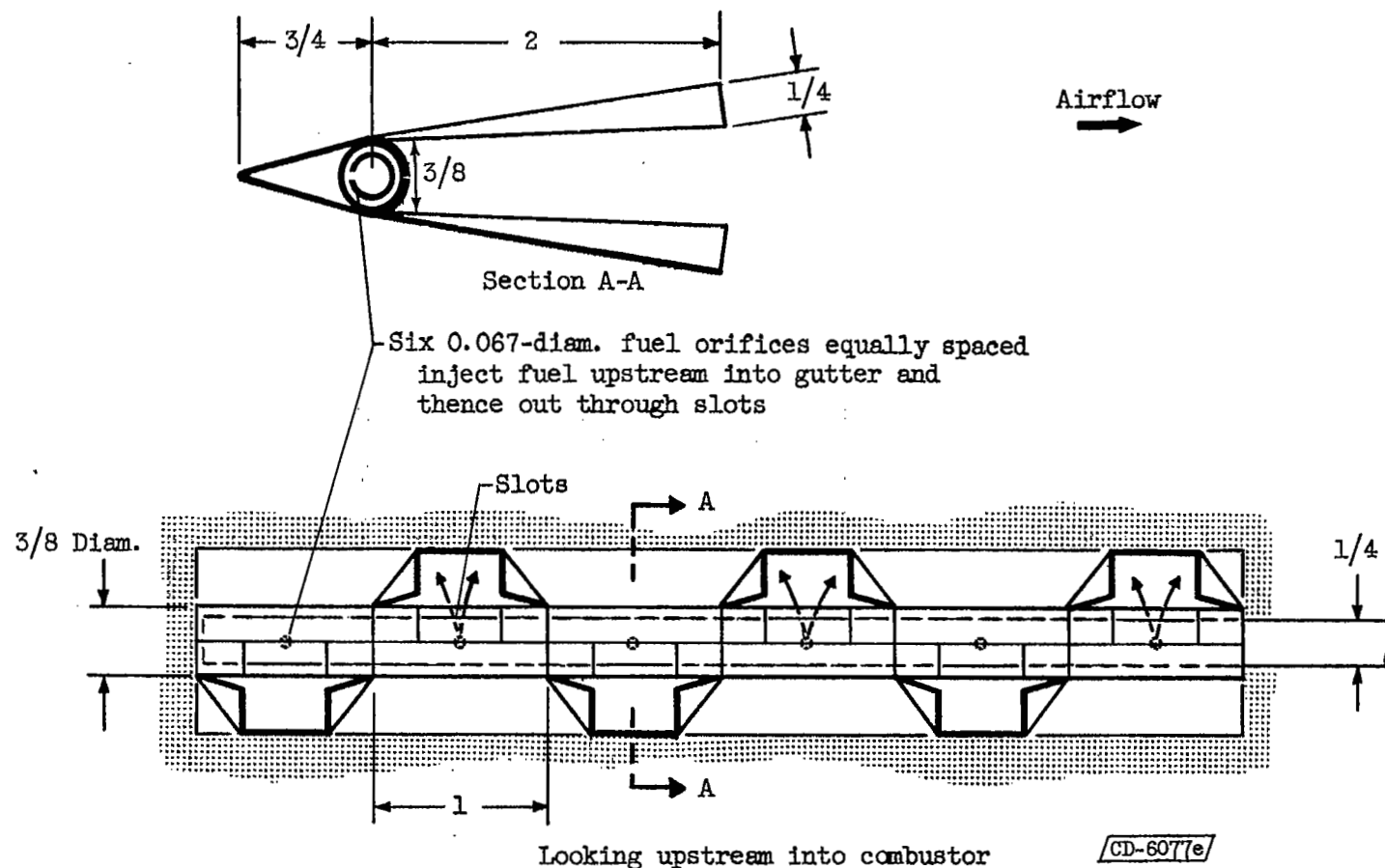


Looking upstream into combustor

CD-6077b

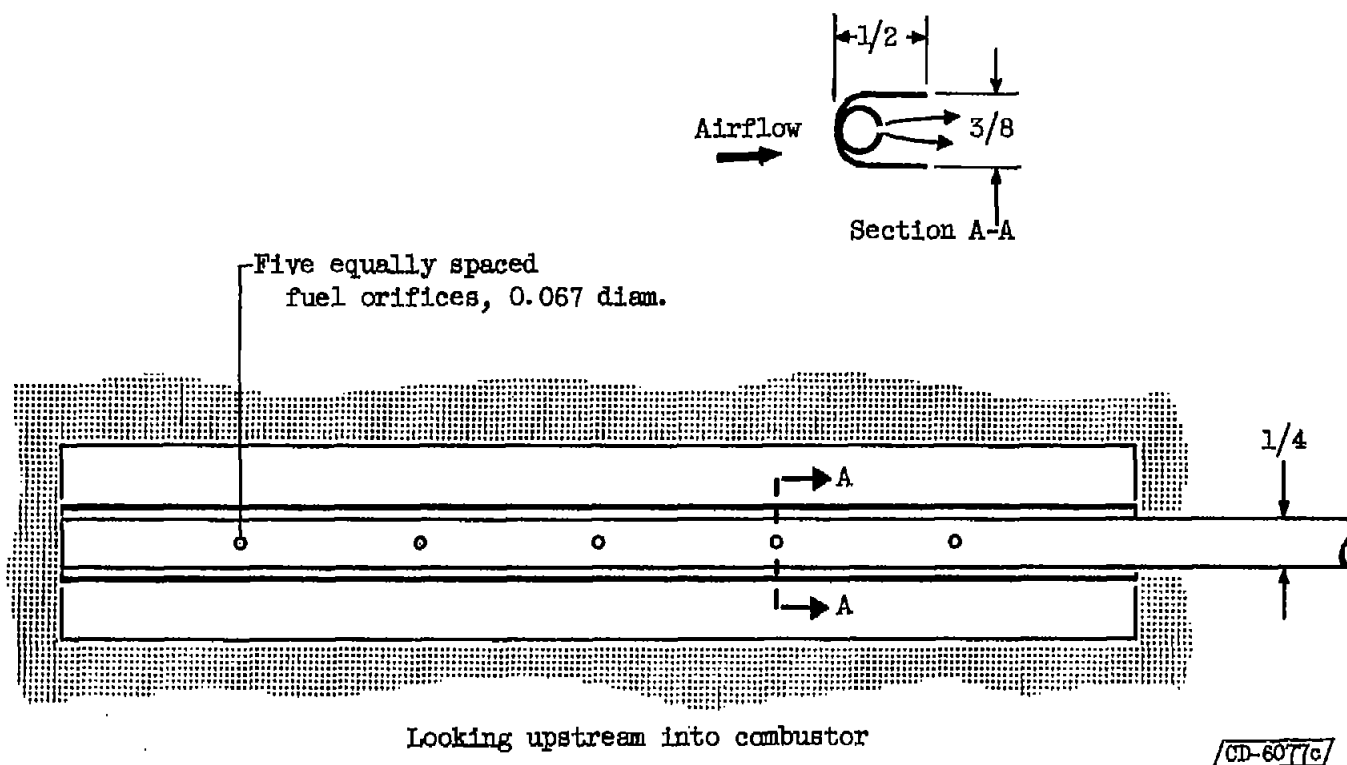
(b) Configuration B, shrouded spray bar.

Figure 4. - Continued. Details of fuel-injector-flameholder configurations tested in 1- by 6-inch rectangular ramjet combustor. (All dimensions in inches.)



(c) Configuration C, extended sloping gutter.

Figure 4. - Continued. Details of fuel-injector-flameholder configurations tested in 1- by 6-inch rectangular ramjet combustor. (All dimensions in inches.)



(d) Configuration D.

Figure 4. - Continued. Details of fuel-injector-flameholder configurations tested in 1- by 6-inch rectangular ramjet combustor. (All dimensions in inches.)

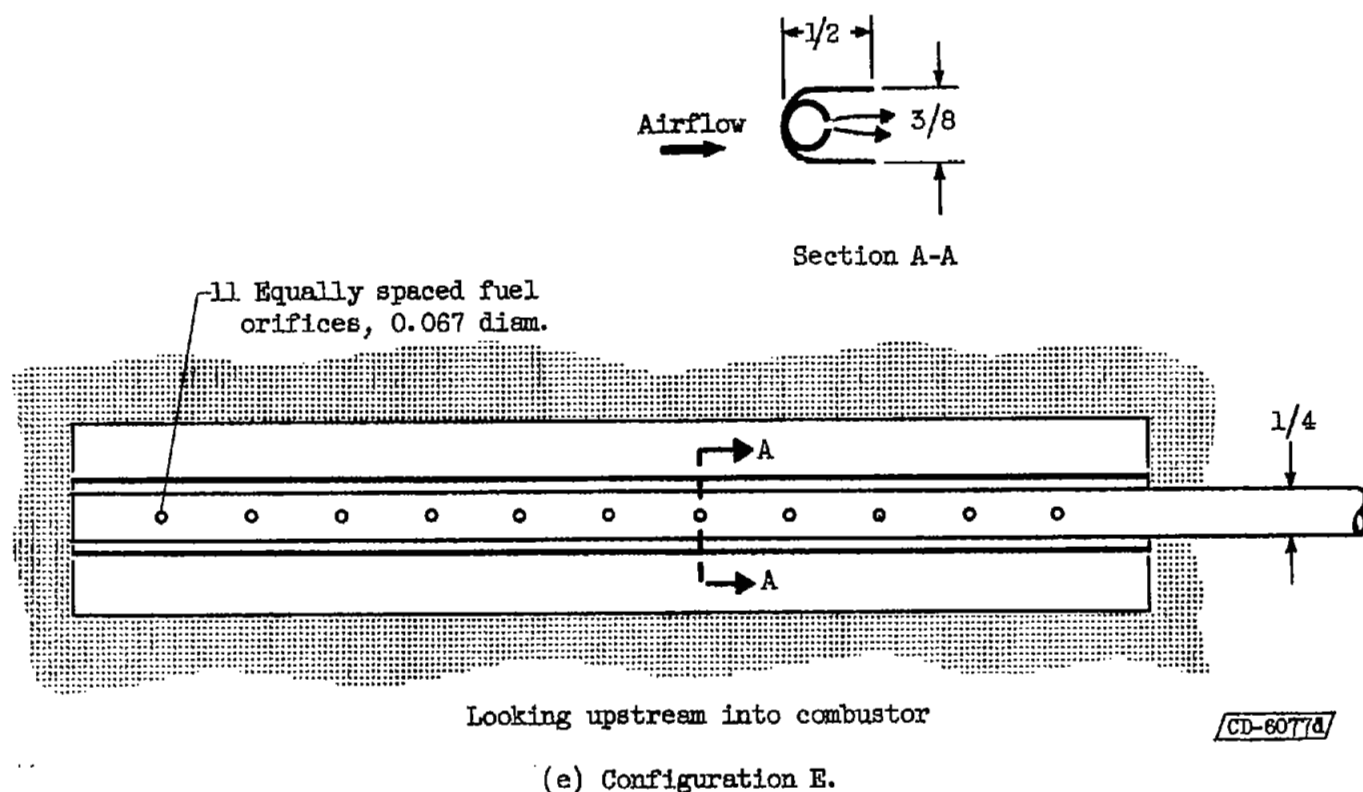
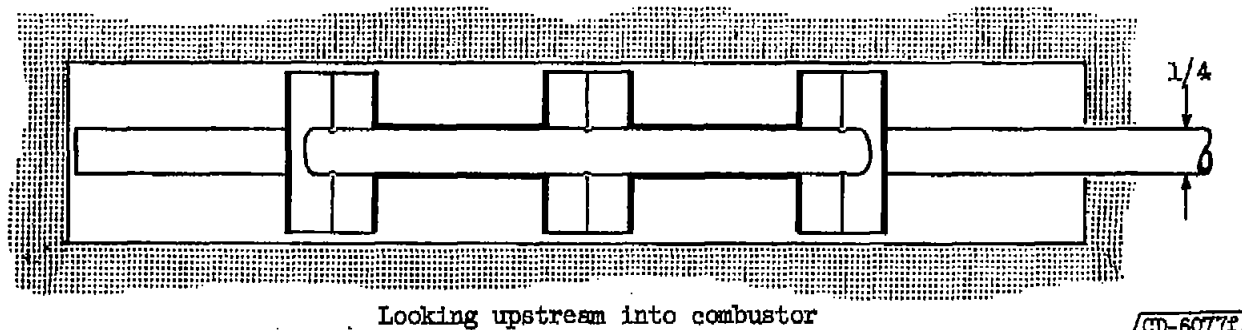
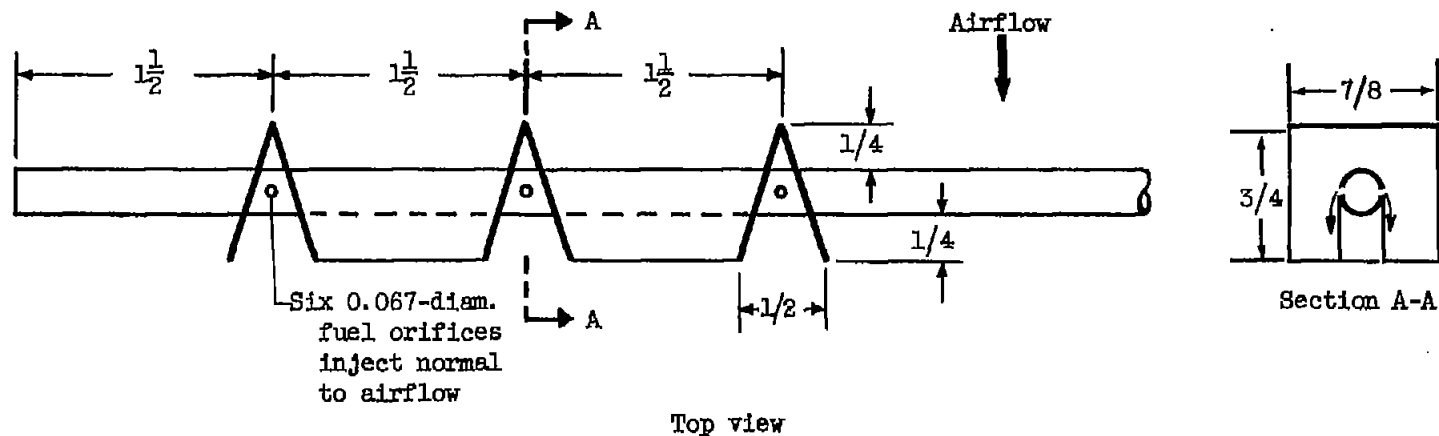
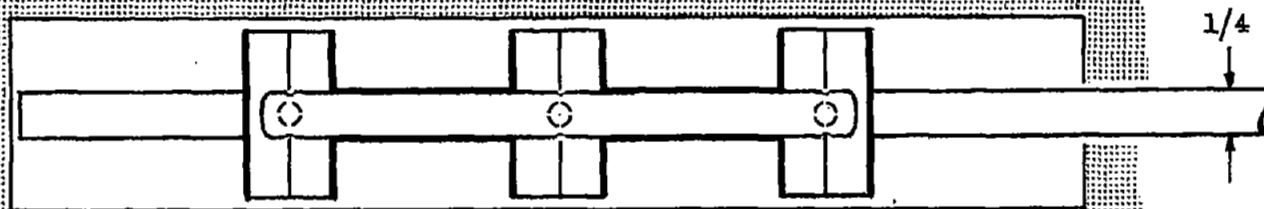
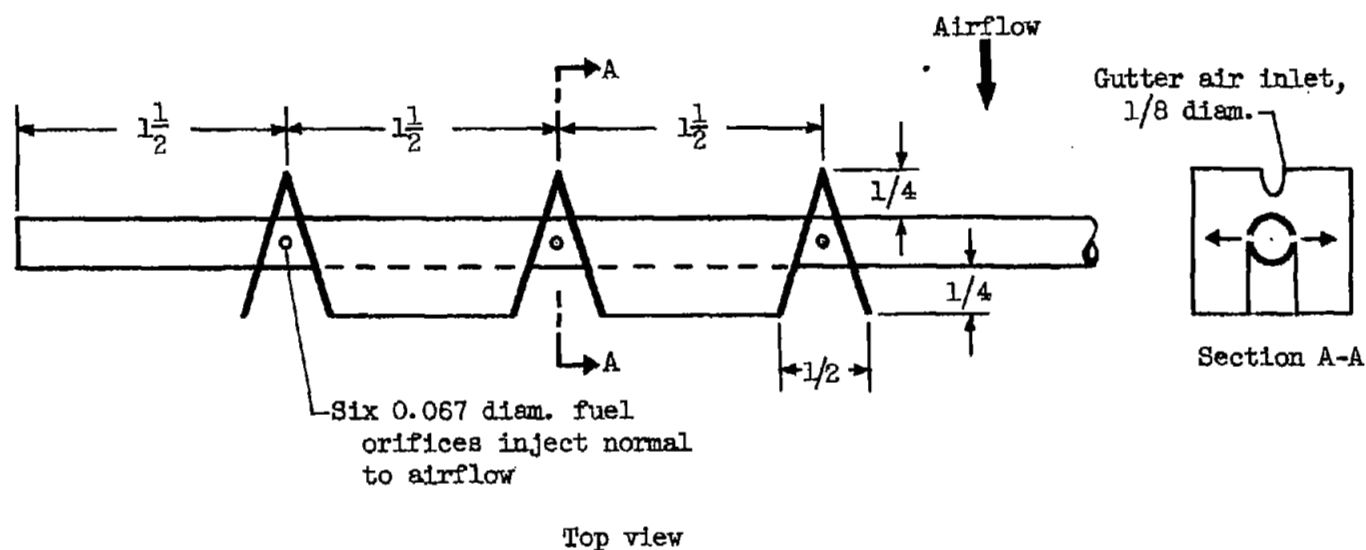


Figure 4. - Continued. Details of fuel-injector-flameholder configurations tested in 1- by 6-inch rectangular ramjet combustor. (All dimensions in inches.)



(f) Configuration F, short V-gutters.

Figure 4. - Continued. Details of fuel-injector-flameholder configurations tested in 1- by 6-inch rectangular ramjet combustor. (All dimensions in inches.)



(g) Configuration G, short V-gutters with air inlet holes.

Figure 4. - Concluded. Details of fuel-injector-flameholder configurations tested in 1- by 6-inch rectangular ramjet combustor. (All dimensions in inches.)

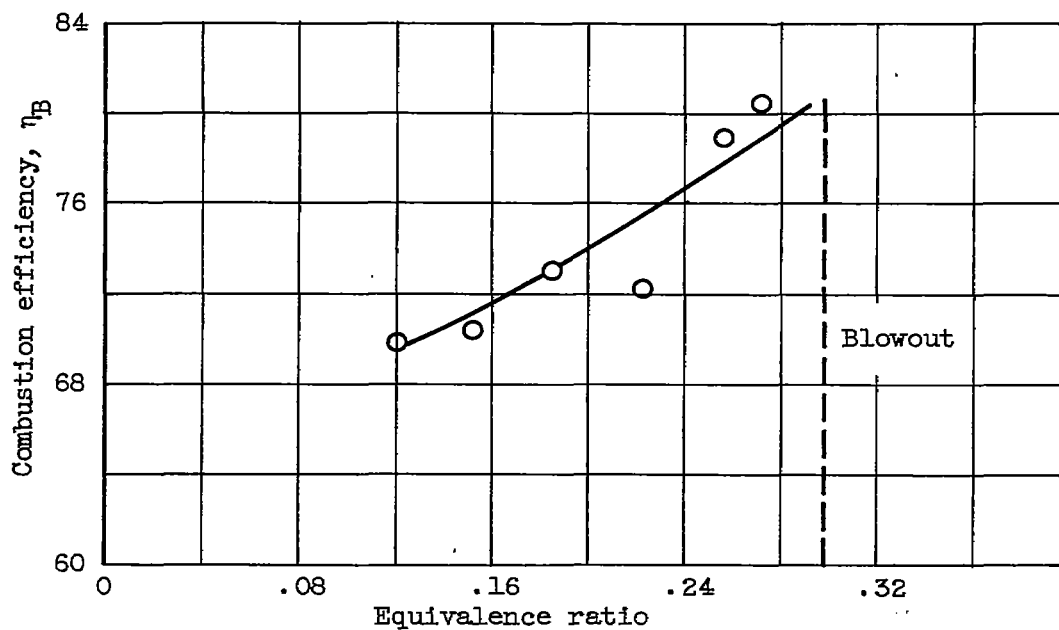
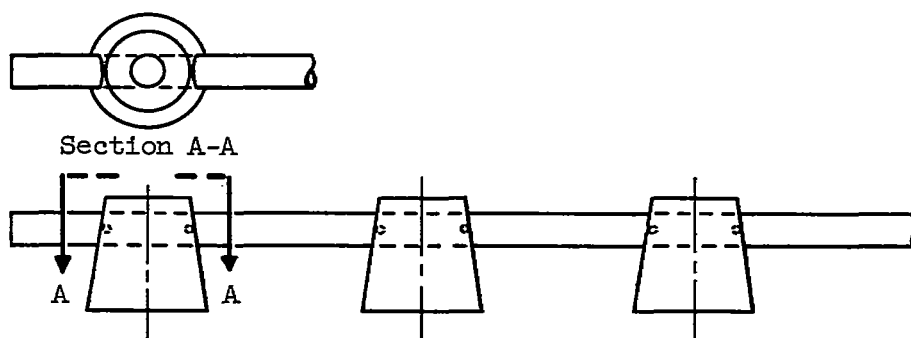


Figure 5. - Combustion efficiency of configuration A. Inlet air pressure, 13.6 ± 0.6 inches of mercury; inlet Mach number, 0.26 ± 0.02 ; inlet temperature, $81^\circ \pm 1^\circ$ F.



View A-A

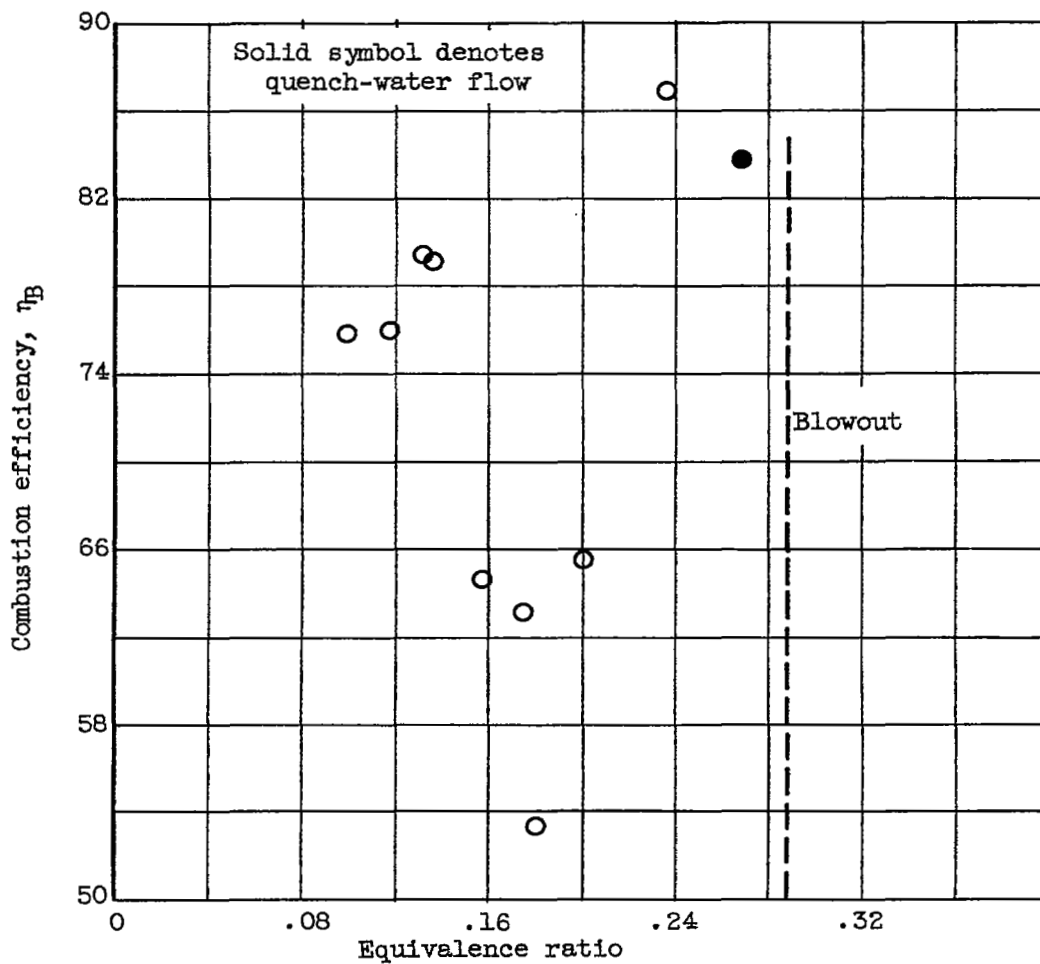
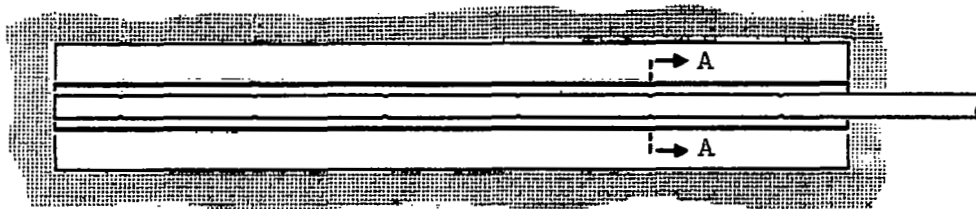
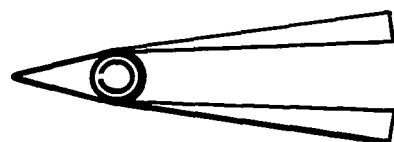


Figure 6. - Combustion efficiency of configuration B. Inlet air pressure, 14.5 ± 0.5 inches of mercury; inlet Mach number, 0.25 ± 0.02 ; inlet temperature, $80^\circ \pm 3^\circ$ F.



Section A-A

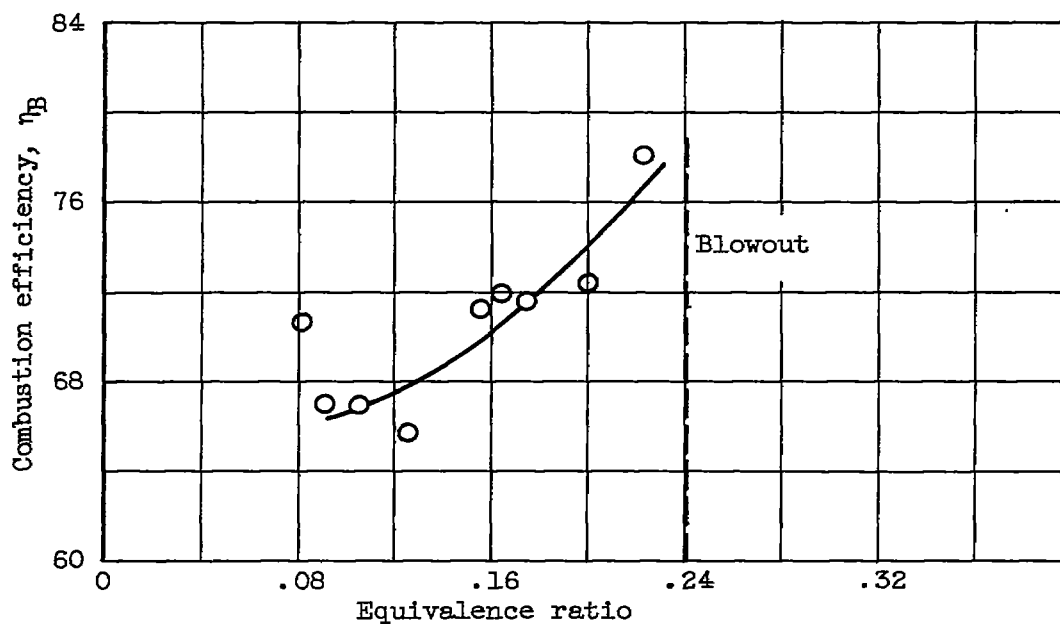
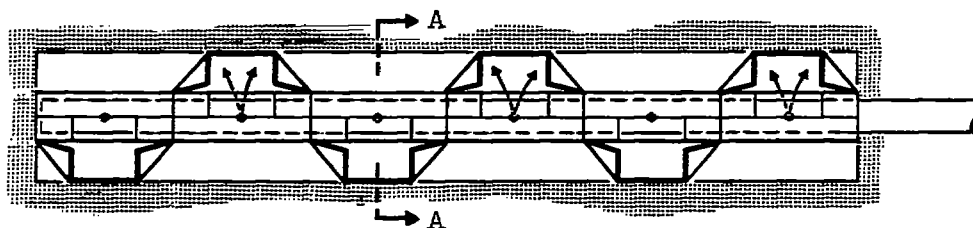


Figure 7. - Combustion efficiency of configuration C. Inlet air pressure, 15.4 ± 0.8 inches of mercury; inlet Mach number, 0.23 ± 0.01 ; inlet air temperature, 80° F.



Section A-A

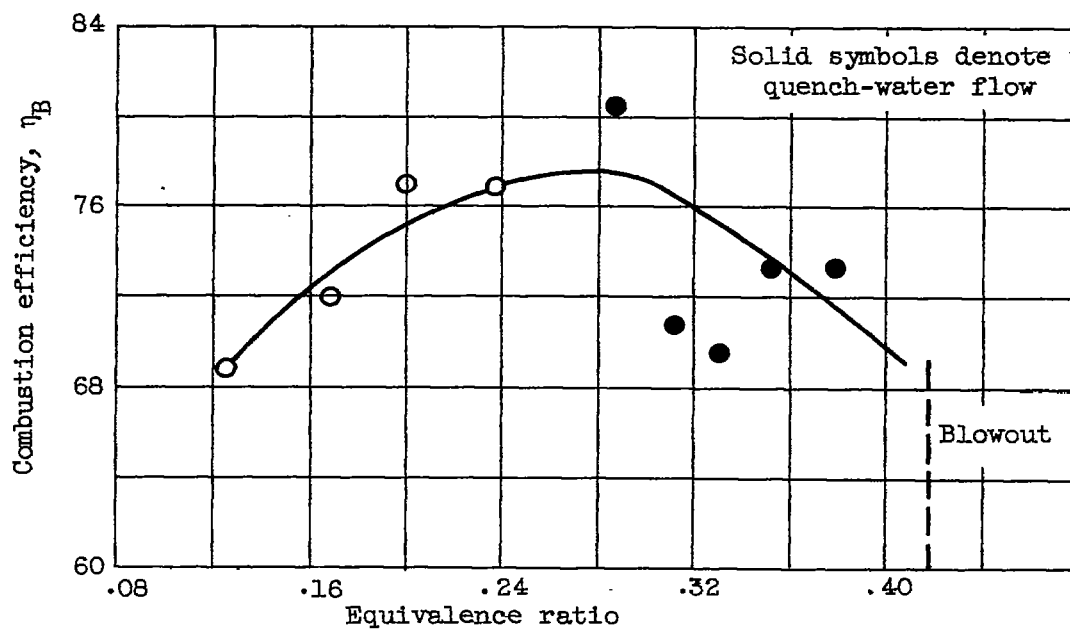
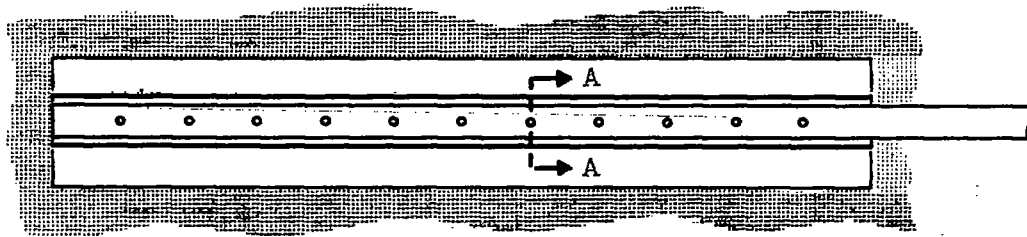


Figure 8. - Combustion efficiency of configuration D. Inlet air pressure, 14.8 ± 0.9 inches of mercury; inlet Mach number, 0.24 ± 0.02 ; inlet temperature, $78^\circ \pm 1^\circ$ F.



Section A-A

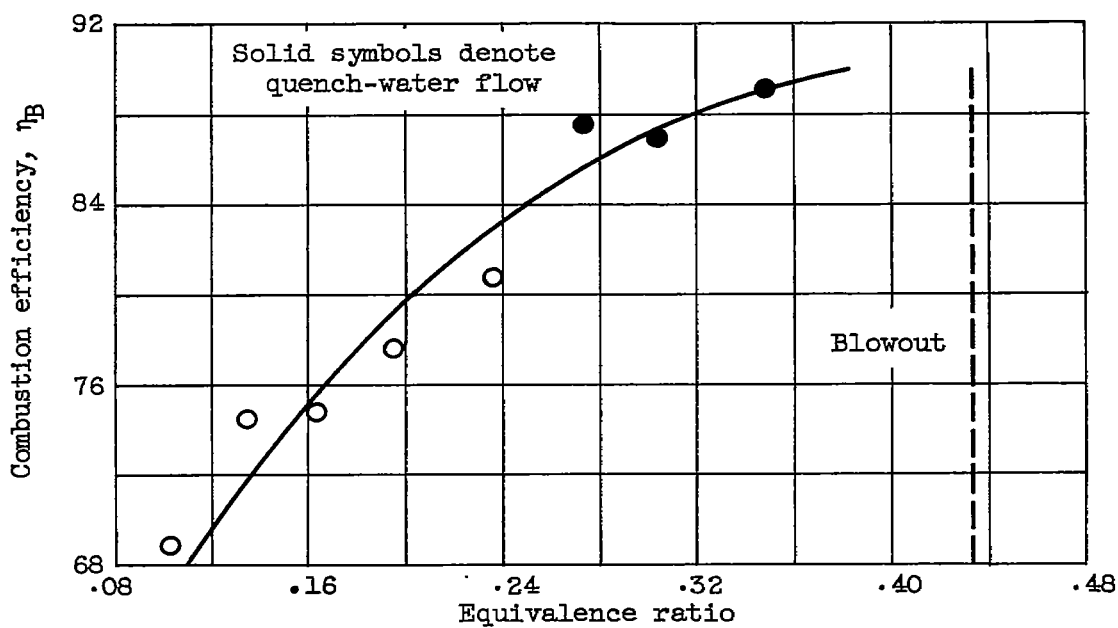
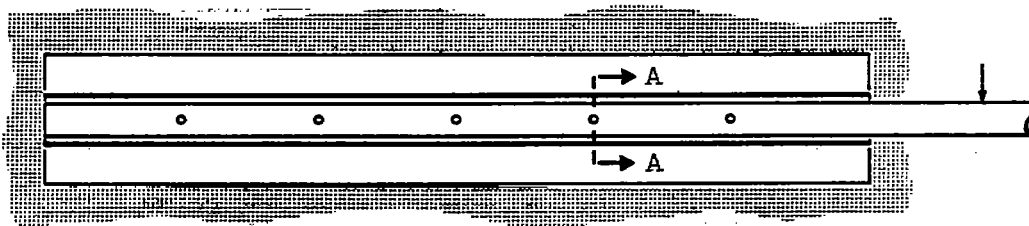
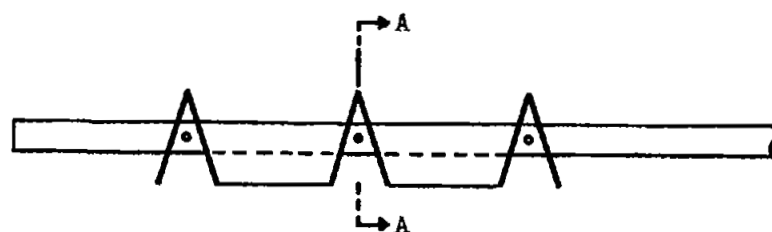


Figure 9. - Combustion efficiency of configuration E. Inlet air pressure, 14.6 ± 0.6 inches of mercury; inlet Mach number, 0.24 ± 0.02 ; inlet temperature, $78^\circ \pm 1^\circ$ F.



Section A-A

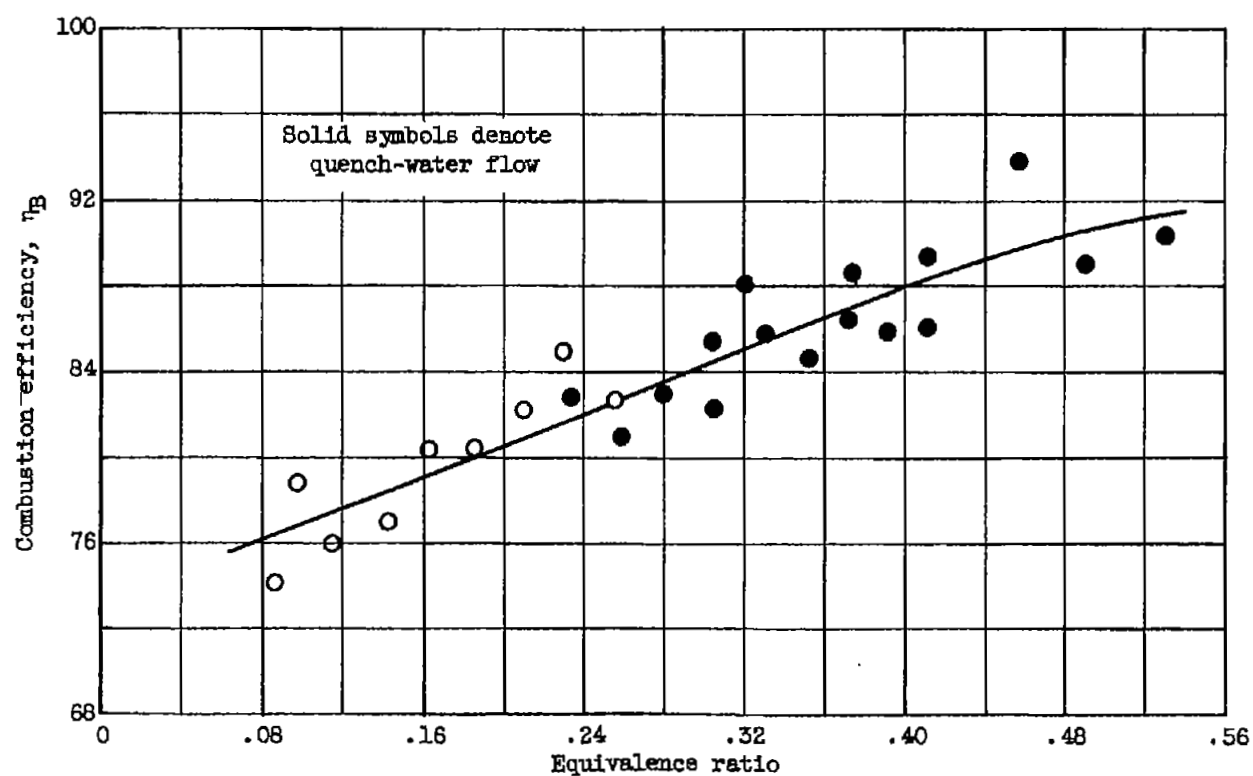


Figure 10. - Combustion efficiency of configuration F. Inlet air pressure, 15.1 ± 1.2 inches of mercury; inlet Mach number, 0.24 ± 0.03 ; inlet temperature, $87^\circ \pm 10^\circ$ F.

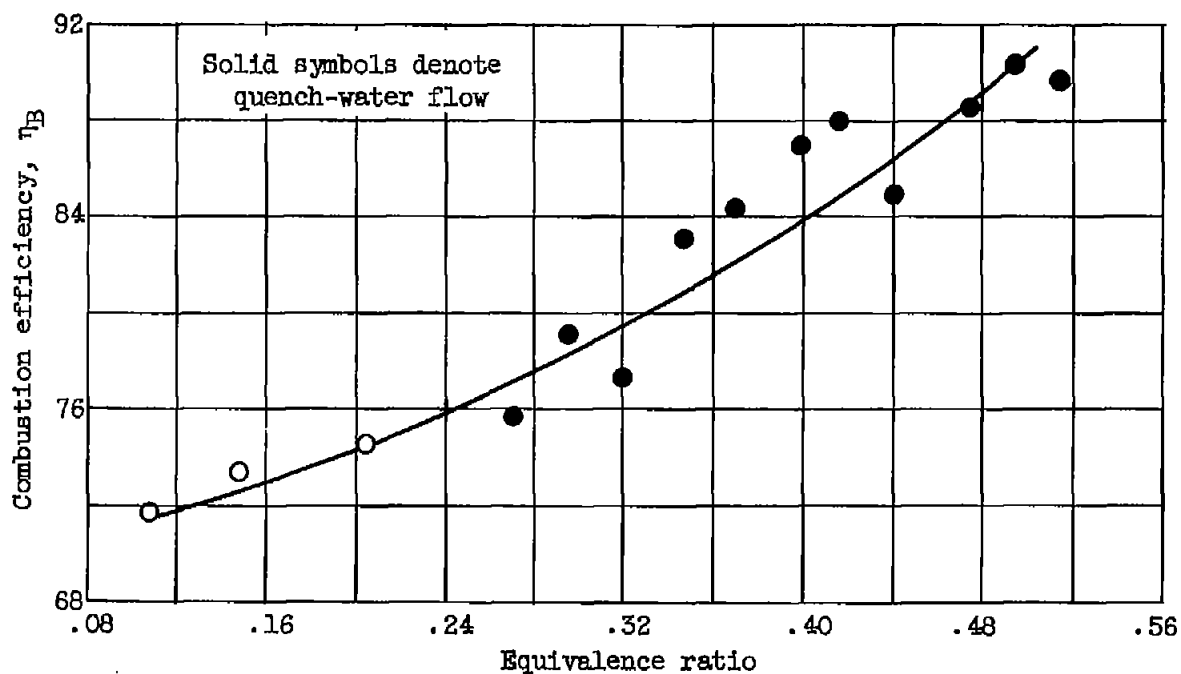
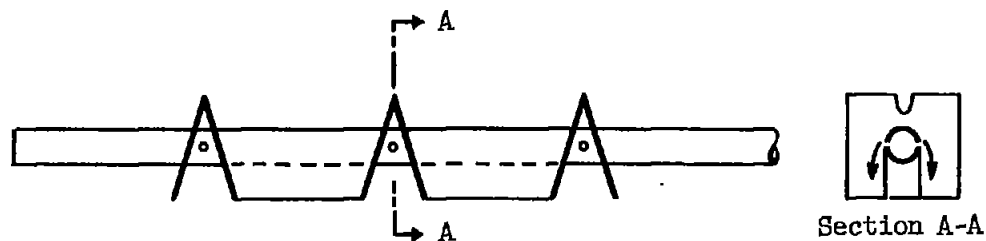
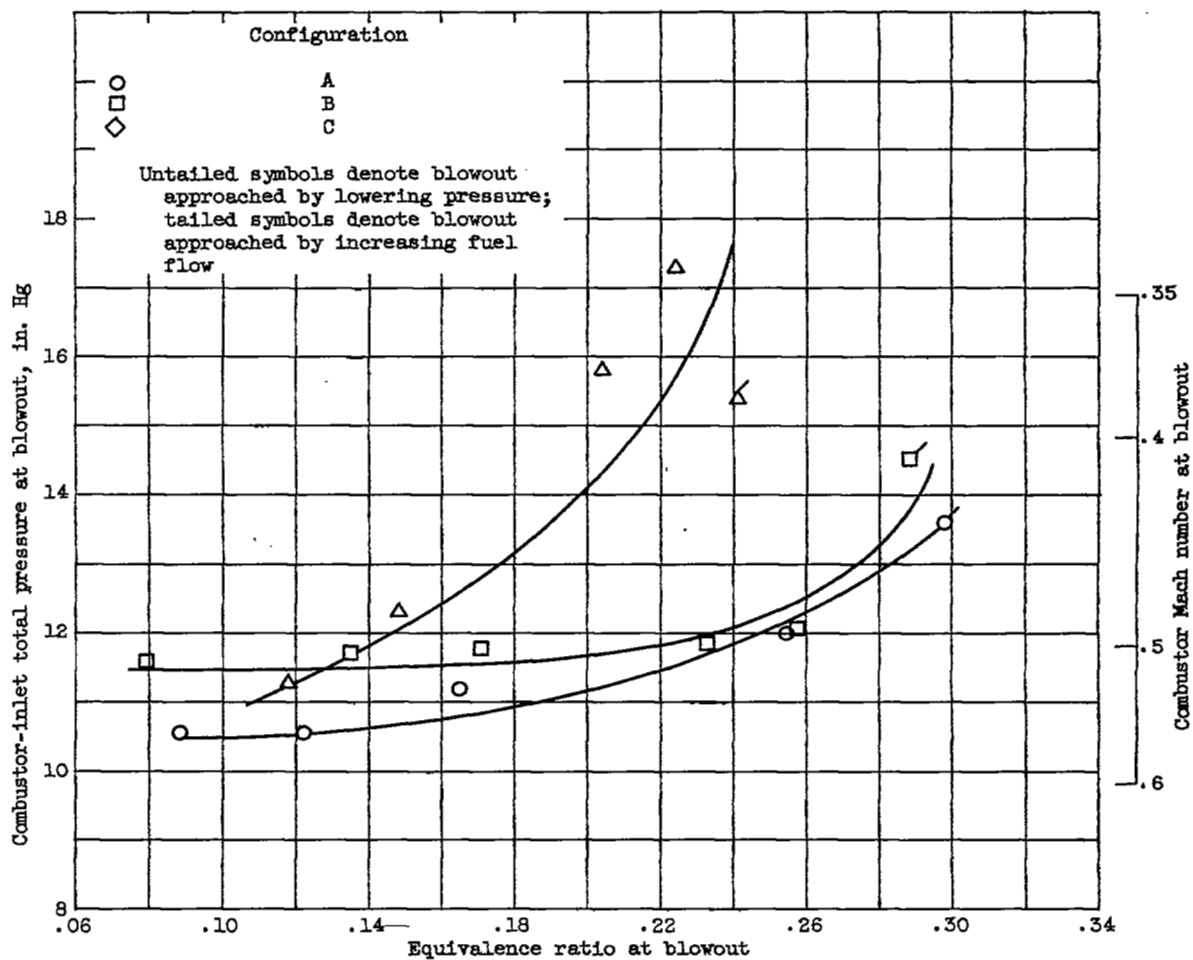
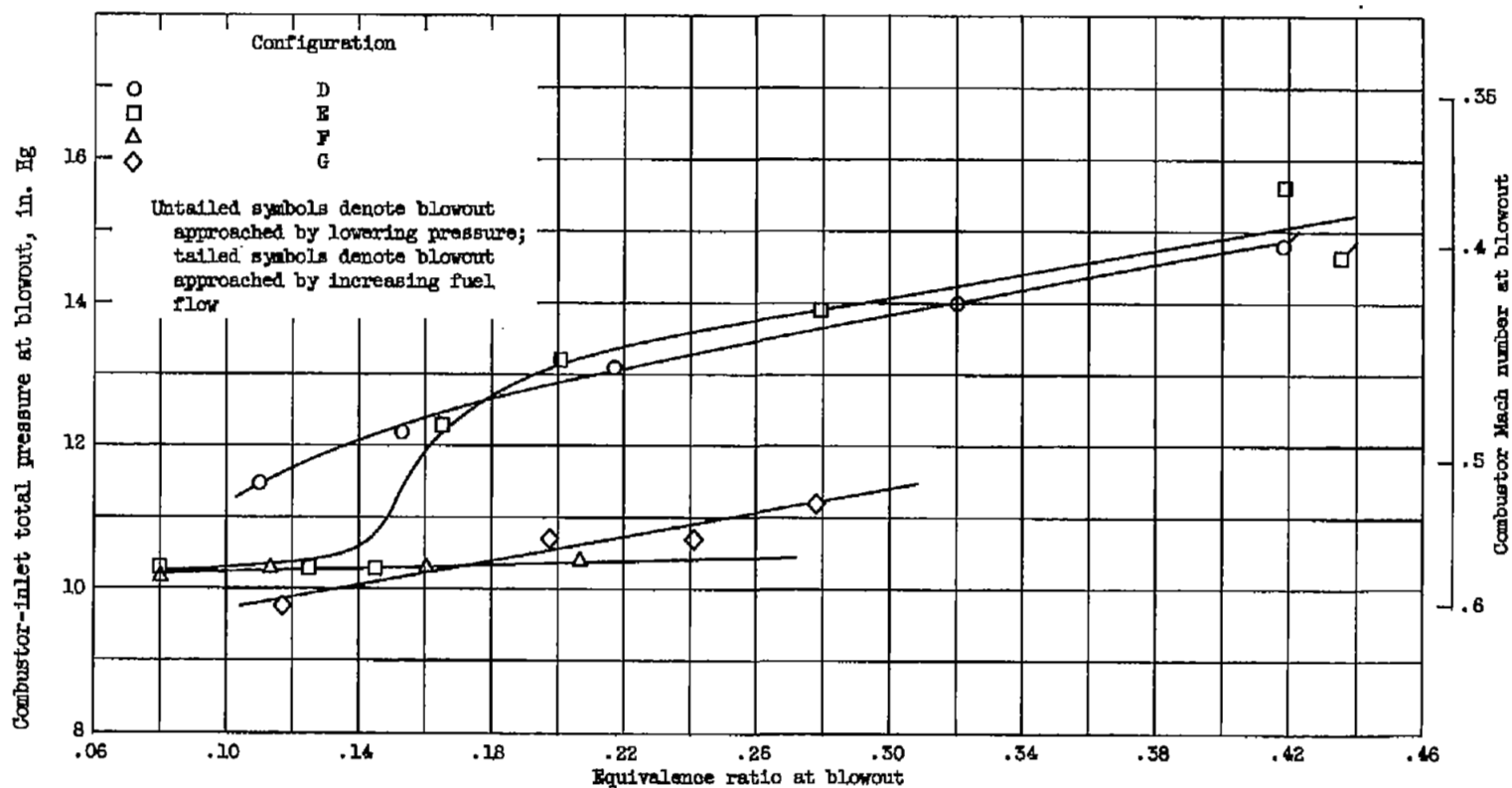


Figure 11. - Combustion efficiency of configuration G. Inlet air pressure, 14.4 ± 1.0 inches of mercury; inlet Mach number, 0.25 ± 0.02 ; inlet temperature, $73^\circ \pm 3^\circ$ F.



(a) Configurations A, B, and C.

Figure 12. - Combustor-inlet total pressure and equivalence ratio at blowout for several configurations. Combustor-inlet total temperature, $80^{\circ} \pm 10^{\circ}$ F; airflow, 0.397 ± 0.008 pound per second.



(b) Configurations D, E, F, and G.

Figure 12. - Concluded. Combustor-inlet total pressure and equivalence ratio at blowout for several configurations. Combustor-inlet total temperature, $80^{\circ} \pm 10^{\circ}$ F; airflow, 0.597 ± 0.008 pound per second.

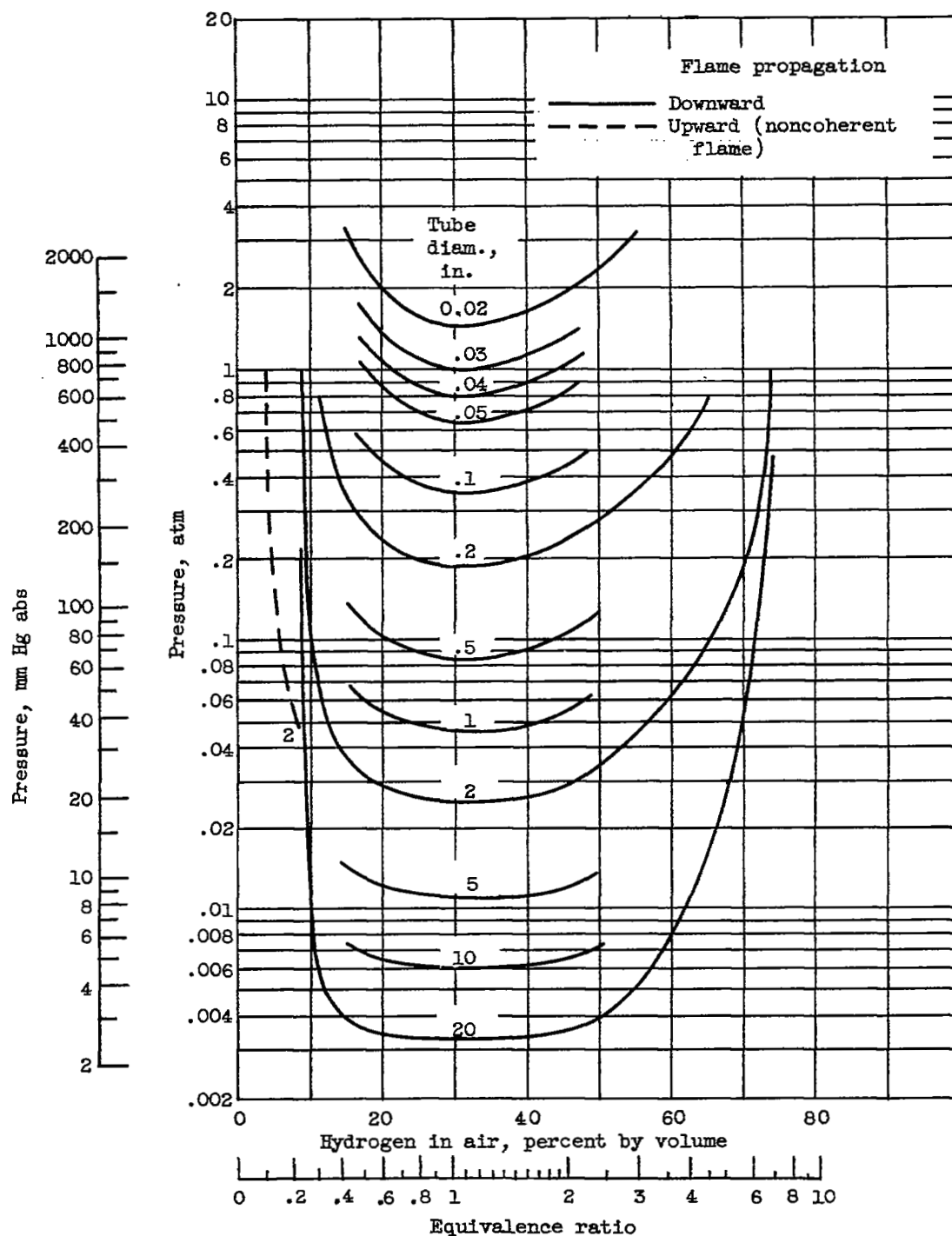


Figure 13. - Estimated pressure limits of flame propagation for hydrogen-air mixtures with various tube diameters. (Reproduced from ref. 4.)

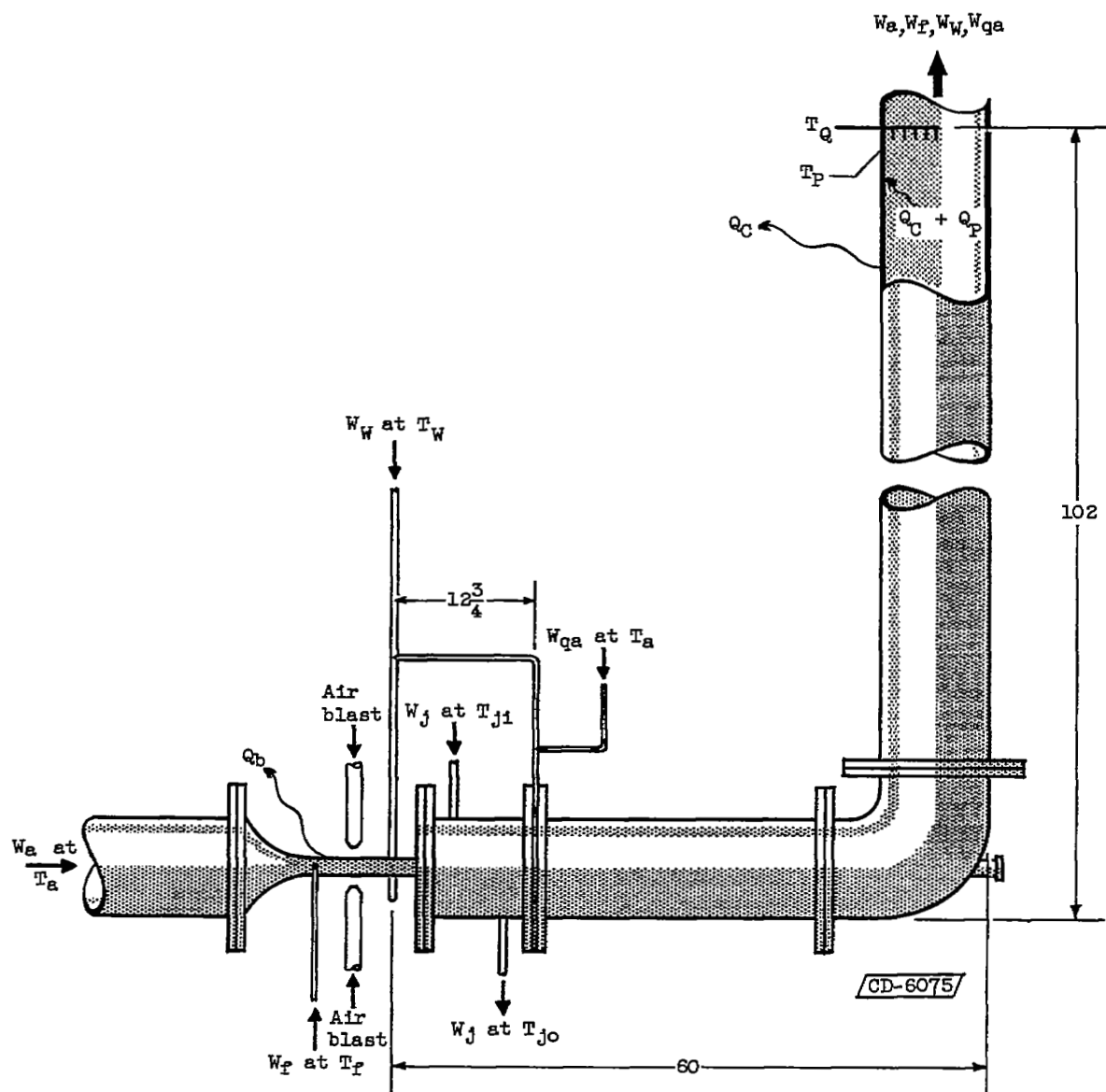


Figure 14. - Combustor-calorimeter heat-balance system. (All dimensions in inches.)

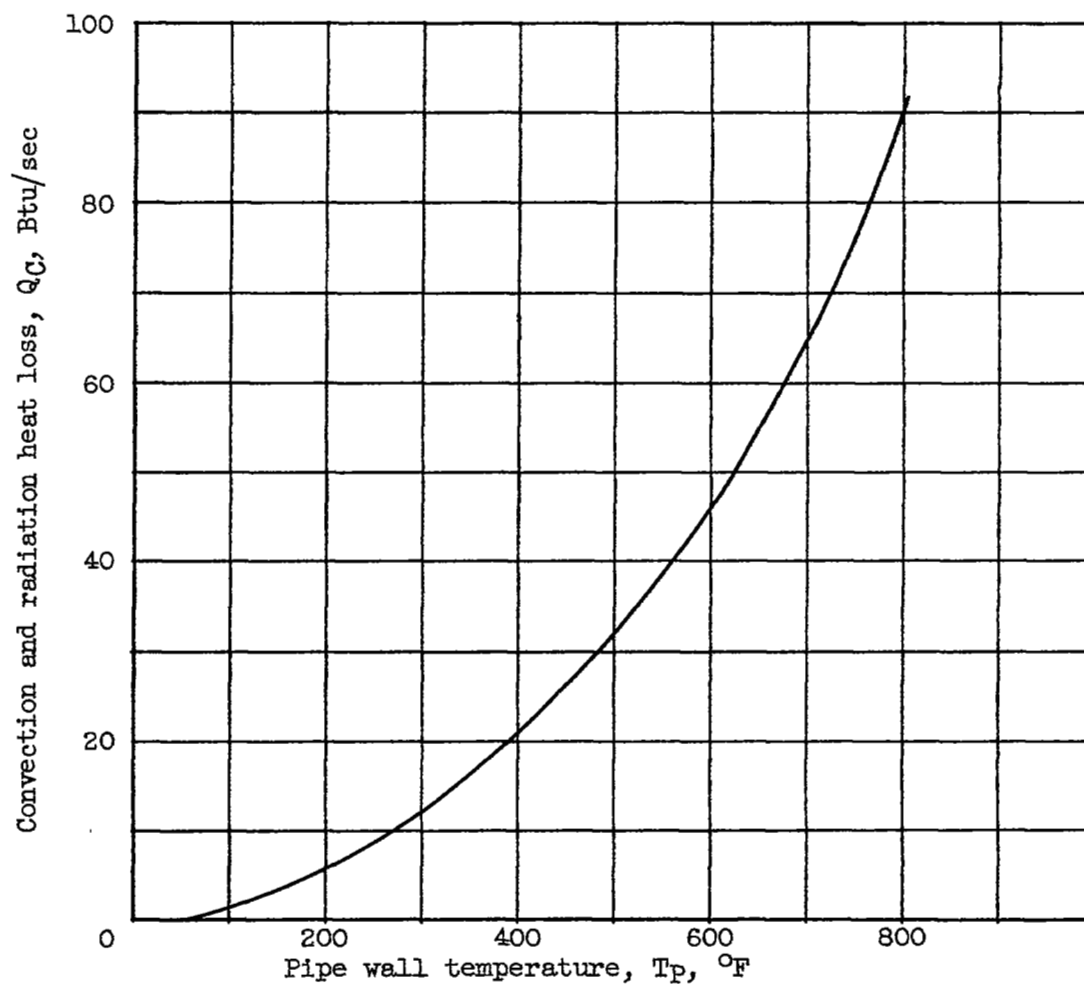


Figure 15. - Convection heat loss from calorimeter piping to room air.

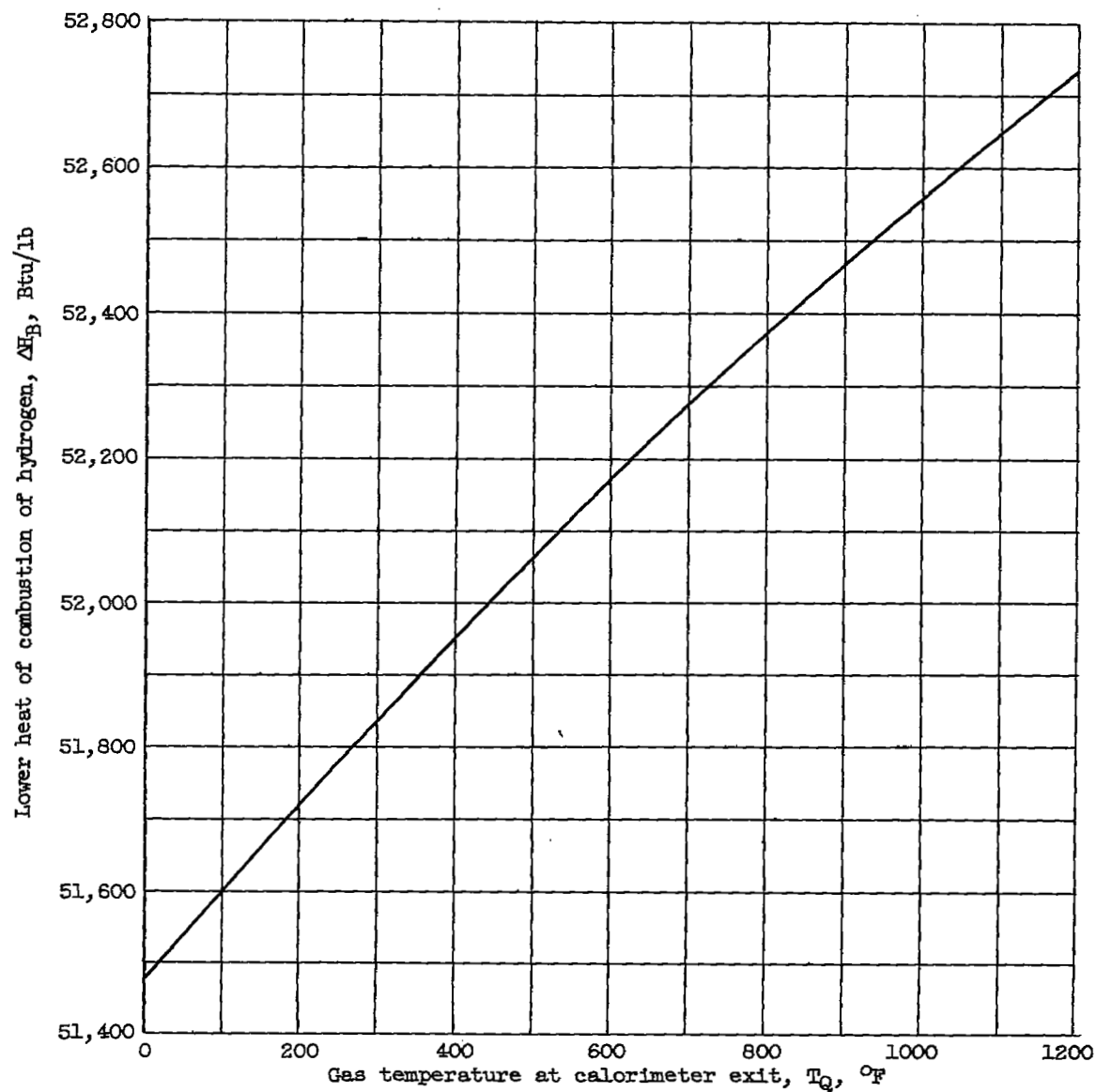


Figure 16. - Lower heat of combustion of hydrogen at 1-atmosphere pressure.

NASA Technical Library



3 1176 01435 9187

~~CONFIDENTIAL~~